Geometric and numerical techniques in optimal control of the two and three-body problems

Bernard Bonnard, Jean-Baptiste Caillau, Gautier Picot

Geometric and numerical techniques in optimal control of the two and three-body problems

B. Bonnard,* J.-B. Caillau† and G. Picot‡

Dedicated to John Baillieul on the occasion of his 65th birthday

Abstract. The objective of this article is to present geometric and numerical techniques developed to study the orbit transfer between Keplerian elliptic orbits in the two-body problem or between quasi-Keplerian orbits in the Earth-Moon transfer when low propulsion is used. We concentrate our study on the energy minimization problem. From Pontryagin's maximum principle, the optimal solution can be found solving the shooting equation for smooth Hamiltonian dynamics. A first step in the analysis is to find in the Kepler case an analytical solution for the averaged Hamiltonian, which corresponds to a Riemannian metric. This will allow to compute the solution for the original Kepler problem, using a numerical continuation method where the smoothness of the path is related to the conjugate point condition. Similarly, the solution of the Earth-Moon transfer is computed using geometric and numerical continuation techniques.

1 Introduction

In this article we consider the orbit transfer in the two and three-body problem, using low propulsion. In the first case, the model is given by Kepler equation

$$\ddot{q} = -\frac{q}{|q|^3} + \frac{u}{m}$$

where m represents the mass of the satellite, subject to

$$\dot{m} = -\delta|u|$$

modelling fuel consumption. The control satisfies the constraint $|u| \leq \varepsilon$ where ε is a small parameter.

The physical optimal control has to maximize the final mass which leads to

$$\min_{u(.)} \int_0^{t_f} |u| \mathrm{d}t$$

*Mathematics Institute, Bourgogne University & CNRS, 9 avenue Savary, F-21078 Dijon (bernard.bonnard@u-bourgogne.fr).

†Same address (jean-baptiste.caillau@u-bourgogne.fr), supported by Conseil Régional de Bourgogne (contract no. 2009-160E-160-CE-160T).

‡Same address (gautier.picot@u-bourgogne.fr), supported by CNRS (contract no. 37244) and Conseil Régional de Bourgogne (contract no. 079201PP02454515).

where t_f is the fixed transfer time. From Pontryagin maximum principle [27], fixing the boundary conditions—*e.g.* a transfer from a low eccentric to a geostationary orbit—, an optimal solution can be numerically computed using a shooting algorithm. This leads to a complicated numerical problem. In [19], the following numerical scheme is proposed. One computes the optimal solution using the convex homotopy

$$\min_{u(.)} \int_0^{t_f} [\lambda |u|^2 + (1-\lambda)|u|] \mathrm{d}t, \quad \lambda \in [0,1],$$

which amounts to regularizing the L^1-minimization problem into an L^2-problem. This was the starting point of the use of continuation methods in orbital transfer, when low propulsion is applied—see also [14] for the use of the continuation method in the time minimal control problem, where the homotopy parameter is the bound of the maximal amplitude of the thrust. From the mathematical point of view, the original dynamics associated with the optimal flow is replaced by another Hamiltonian one, and a continuation is made to solve the shooting equation.

The first motivation of this article is to present a neat geometric result from [8]: Neglecting the mass variation, restricting to coplanar transfer (the inclination being considered as a homotopy parameter) and replacing the L^1-problem by an averaged L^2-problem, one can substitute the Hamiltonian vector field defined by the maximum principle with

$$H = \frac{1}{2n^{5/3}} \left[9n^2 p_n^2 + \frac{5}{2}(1-e^2) p_e^2 + \frac{5-4e^2}{2} \frac{p_\theta^2}{e^2} \right],$$

where n is the mean motion, e the eccentricity, and θ the angle of the pericenter (the singularity $e = 0$ corresponds to circular orbits). Coordinates (n, e, θ) are moreover orthogonal coordinates for the Riemannian metric associated with H,

$$g = \frac{\mathrm{d}n^2}{9n^{\frac{1}{3}}} + \frac{2n^{\frac{5}{3}}}{5(1-e^2)} \mathrm{d}e^2 + \frac{2n^{\frac{5}{3}}}{5-4e^2} \mathrm{d}\theta^2.$$

Such a metric is isometric to

$$g = \mathrm{d}r^2 + \frac{r^2}{c^2} (\mathrm{d}\varphi^2 + G(\varphi) \mathrm{d}\theta^2)$$

where

$$r = \frac{2}{5} n^{5/6}, \quad \varphi = \arcsin e$$

and

$$c = \sqrt{2/5}, \quad G(\varphi) = \frac{5 \sin^2(\varphi)}{1 + 4\cos^2(\varphi)}.$$

The Hamiltonian flow $\overrightarrow{H}$ is Liouville integrable and the metric in the above normal form captures the main properties of the averaged orbital transfer. Indeed, one can extract from g the following two-dimensional Riemannian metrics:

- $g_1 = \mathrm{d}r^2 + r^2 \mathrm{d}\psi^2$ which is associated with the orbital transfer where θ is kept fixed (this encompasses the case of circular targets). Such a metric is flat and geodesics are straight lines in suitable coordinates.

– $g_2 = \mathrm{d}\varphi^2 + G(\varphi)\mathrm{d}\theta^2$ which represents the restriction of the metric to $r^2 = c^2$ and describes by homogeneity the orbit transfer in the general case.

A generalization of the results of [30] will allow to compute for the metric g_2 the conjugate and cut loci and to get a global optimality solution for the averaged optimal control problem. This is the starting point to analyze the original optimal control problem using a continuation method.

A second motivation of this article is to present some results from geometric control theory connected to our analysis with adapted numerical codes developed to compute the solutions. First of all, the maximum principle is only a necessary optimality condition. In order to get sufficient optimality conditions under generic assumptions one must define the concept of conjugate point, associated with the energy minimization problem. This concept was already introduced in the standard litterature of calculus of variations [5]. If the Hamiltonian optimal dynamics is described by a smooth Hamiltonian vector field $\overrightarrow{H}$, conjugate points are the image of the singularities of the exponential mapping: $\exp_{x(0)} : p(0) \longrightarrow \Pi_x \exp t_f \overrightarrow{H}(x(0), p(0))$ where $\Pi_x : (x, p) \longrightarrow x$ is the canonical projection. Such points can be numerically computed using the code [12]. An important remark, in view of the use of the (smooth) continuation method in optimal control is to observe that the shooting equation is precisely to find $p(0)$ such that $\exp_{x(0)}(p(0)) = x_1$ where x_1 is the terminal condition and the derivative is generated using the variational equation of $\overrightarrow{H}$. This will lead to convergence results for the smooth continuation method in optimal control, related to estimates of conjugate points.

The last section is devoted to the Earth-Moon transfer, using low propulsion. The model is the standard circular restricted model [24] where the two primaries are fixed in a rotating frame. Up to a normalization the system can be written in Hamiltonian form,

$$\dot{x} = \overrightarrow{H_0}(x) + u_1\overrightarrow{H_1}(x) + u_2\overrightarrow{H_2}(x)$$

where $x = (q, p) \in \mathbf{R}^4$ and the drift $\overrightarrow{H_0}$ is given by

$$H_0(x) = \frac{1}{2}(p_1^2 + p_2^2) + p_1q_2 - p_2q_1 - \frac{1-\mu}{\rho_1} - \frac{\mu}{\rho_2}\,,$$

q being the position of the spacecraft, ρ_1 representing the distance to the Earth with mass $1-\mu$ located at $(-\mu, 0)$, and ρ_2 the distance to the Moon with mass μ located at $(1-\mu, 0)$, $\mu \simeq 1.2153e-2$ being a small parameter. The Hamiltonian fields associated with the control are given by

$$H_i(x) = -q_i, \quad i = 1, 2,$$

and the control bound is $|u| \leq \varepsilon$. The parameter μ is small and this remark was used by Poincaré to study the dynamics of the free motion described by $\overrightarrow{H_0}$ by making a deformation of the case $\mu = 0$ which corresponds to Kepler equation in rotating coordinates [24]. Inspired by this approach and using our preliminary geometric analysis, we propose a simple solution to the Earth-Moon transfer using low propulsion for the energy minimization problem.

2 Geometric and numerical methods

2.1 Maximum principle

We consider the energy minimization problem $\min_{u(.)} \int_0^{t_f} |u|^2 \mathrm{d}t$, for a smooth control system of the form

$$\dot{x} = F_0(x(t)) + \sum_{i=1}^{m} u_i(t) F_i(x(t)) = F(x(t), u(t)), \quad x \in X.$$

The set of admissible controls is the subset $\mathcal{U}$ of measurable bounded mappings $u(.)$ with corresponding trajectory $x(.)$ defined on the whole interval $[0, t_f]$. Pontryagin maximum principle [27] tells us that

Proposition 2.1. *If (x, u) is an optimal pair on $[0, t_f]$, there exists a non trivial pair (p^0, p), $p^0 \leq 0$ and p an absolutely continuous adjoint vector valued in T^*X, such that on $[0, t_f]$ we have*

$$\dot{x} = \frac{\partial H}{\partial p}(x, p, u), \quad \dot{p} = -\frac{\partial H}{\partial x}(x, p, u), \tag{1}$$

and

$$H(x, p, u) = \max_{v \in \mathbf{R}^m} H(x, p, v) \tag{2}$$

where $H(x, p, u) = p^0 \sum_{i=1}^m u_i^2 + < p, F(x, u) >$.

Definition 2.1. The mapping H from $T^*X \times \mathbf{R}^m$ to $\mathbf{R}$ is called the *pseudo-Hamiltonian*. A triple (x, p, u) solution of (1-2) is called an *extremal trajectory*.

2.2 Computation of extremals

From the maximization condition (4), one deduces that $\partial H/\partial v = 0$, and there are two types of extremals:

- *Abnormal extremals.* They correspond to the situation $p^0 = 0$ and are implicitely defined by the relations $H_i = 0$, $i = 1, \ldots, m$, where $H_i =< p, F_i(x) >$ are the Hamiltonian lifts.
- *Normal extremals.* If $p^0 < 0$, it can be normalized to $-1/2$ by homogeneity. From $\partial H/\partial v = 0$, one deduces $u_i = H_i$ for $i = 1, \ldots, m$, and plugging such H_i into H defines a true smooth Hamiltonian

  $$H_n = H_0 + \frac{1}{2} \sum_{i=1}^{m} H_i^2$$

  whose solutions are the *normal extremals*.

2.3 The concept of conjugate point

Definition 2.2. Let $z = (x, p)$ be a normal reference extremal defined on $[0, t_f]$. The variational equation

$$\dot{\delta} z(t) = \mathrm{d}\overrightarrow{H_n}(z(t)) \delta z(t)$$

is called the *Jacobi equation*. A *Jacobi field* is a non-trivial solution $\delta z = (\delta x, \delta p)$. It is said to be *vertical* at time t if $\delta x(t) = \mathrm{d}\Pi_x(z(t))\delta z(t) = 0$ where Π_x is the projection $(x,p) \mapsto x$.

The following standard geometric result is crucial.

Proposition 2.2. *Let L_0 be the fiber $T^*_{x_0}X$ and $L_t = \exp_t(\overrightarrow{H_n})(L_0)$ be its image by the one-parameter subgroup generated by $\overrightarrow{H}_n$. Then L_t is a Lagrangian submanifold whose tangent space at $z(t)$ is generated by the Jacobi fields which are vertical at $t = 0$.*

Definition 2.3. We fix $x_0 = x(0)$ and define for $t \in [0, t_f]$ the *exponential mapping*

$$\exp_{x_0,t}(p_0) = \Pi_x(z(t, z_0))$$

where $z(t, z_0)$, with $z_0 = (x_0, p_0)$, denotes the normal extremal departing from z_0 when $t = 0$.

Definition 2.4. Let $z = (x, p)$ be the reference normal extremal. The time $t_c \in [0, t_f]$ is called *conjugate* if the mapping $\exp_{x_0,t_c}$ is not an immersion at $p(0)$. The associated point $x(t_c)$ is said to be conjugate to x_0. We denote by $t_{1,c}$ the first conjugate point and by $C(x_0)$ the *conjugate locus* formed by the set of first conjugate points when we consider all normal extremals starting from x_0.

The conjugate time notion admits the following generalization.

Definition 2.5. Let M_1 be a regular submanifold of M, and let us define $M_1^\perp = \{(x,p) \in T^*M \mid x \in M_1,\ p \perp T_xM_1\}$. Then $t_{\mathrm{foc}} \in [0, t_f]$ is called a *focal time* if there exists a Jacobi field $J = (\delta x, \delta p)$ such that $\delta x(0) = 0$ and $J(t_{\mathrm{foc}})$ is tangent to $M_1^\perp$.

Remark 2.1. The concept of conjugate point is related to the necessary and sufficient optimality conditions, under generic assumptions, see for instance [12].

2.4 Conjugate points and smooth continuation method

Smooth continuation is a general numerical method to solve a system of equations $F(x) = 0$ where $F : \mathbf{R}^n \longrightarrow \mathbf{R}^n$ is a smooth mapping, see [1]. The principle is to construct a homotopy path $h(x, \lambda)$ such that $h(x, 0) = G(x)$ and $h(x, 1) = F(x)$ where $G(x)$ is a map having known zeros, or where the zeros can be easily computed using a Newton type algorithm. The zeros along the path can be calculated by different methods, the simplest being a discretization $0 = \lambda_0 < \lambda_1 < \cdots < \lambda_n = 1$ of the homotopy parameter where, at step $i+1$, the zero computed at step i is used to initialize Newton algorithm. The approach has to be adapted to optimal control problems: The shooting equation comes from the projection of a symplectic mapping, the Jacobian can be computed using Jacobi fields and one must consider the *central extremal fields* associated with the problem (see [13]). A short description of the method is given below in our case study.

2.4.1 Shooting equation

We consider a family H_λ, $\lambda \in [0,1]$, of smooth Hamiltonians on T^*X associated with normal extremals of an energy minimization problem. We fix the boundary conditions x_0, x_1 and the transfer time t_f. This leads to a family $\exp^\lambda_{x_0,t_f}(p_0)$ of exponential mappings. Using the notation $E^\lambda : p_0 \longrightarrow \exp^\lambda_{x_0,t_f}(p_0)$, one must solve the shooting equation $E^\lambda(p_0) = x_1$.

Proposition 2.3. *For each λ, the shooting equation is of maximal rank if and only if the point x_1 is not conjugate to x_0 for the corresponding λ. Moreover, in this case, the solutions of the shooting equation contain a smooth branch, which can be parameterized by λ and the derivative E'^λ can be generated integrating the Jacobi equation.*

From the above proposition, to ensure convergence of the method one must control

- the distance to the conjugate loci,
- that the branch has is defined on the whole interval $[0,1]$.

The second point is related to two standard problems in optimal control: Existence of Lipschitzian minimizers—hence solutions of the maximum principle [21]—, and compactness of the domain of the exponential mapping. Next we present a nice geometric situation for which convergence of the method is ensured.

Definition 2.6. Consider the normal extremal field $\overrightarrow{H_n}$ of an energy minimization problem with fixed final time t_f. Given an initial condition x_0, the *separating locus* $L(x_0)$ is the set of points where two distinct normal extremal curves intersect with same cost. The *cut point* along a normal extremal is the first point where it ceases to be optimal. The *cut locus* $\mathrm{Cut}(x_0)$ is the set of such points when we consider all extremals initiating from x_0 and losing optimality exactly at time t_f.

2.4.2 Convergence of the continuation method in the Riemannian case

We first recall that the Riemannian problem can be, at least locally, reset in the following framework.

Let $F_1, \ldots, F_n$ be a set of smooth vector fields on a manifold X and assume that they are linearly independent. One can define a Riemannian metric on X by asserting that $\{F_1, \ldots, F_n\}$ form an orthonormal frame. Introducing the control system $\mathrm{d}x(t)/\mathrm{d}t = \sum_{i=1}^n u_i(t) F_i(x(t))$, the length of the curve $x(\cdot)$ is $l(x) = \int_0^T \sum_{i=1}^n (u_i^2(t))^{1/2} \mathrm{d}t$. From Maupertuis principle, minimizing length is equivalent to minimizing the energy $\int_0^T \sum_{i=1}^n u_i^2(t) \mathrm{d}t$. There exists only normal extremals and H_n is given by $(1/2)\sum_{i=1}^n H_i^2$. Fixing the level set $H_n = 1/2$ parameterizes trajectories by arc length. For the energy minimization problem, the transfer time can be arbitrarily prescribed.

Theorem 2.1. *Let g_λ, $\lambda \in [0,1]$, be a smooth family of complete Riemannian metrics on X. Let us fix the initial point x_0. Denote $i_\lambda(x_0)$ the distance from x_0 to the cut locus $\mathrm{Cut}^\lambda(x_0)$ and by $i_\lambda = \inf_{x_0} i_\lambda(x_0)$ the injectivity radius of the corresponding metric. Then,*

– *for length shorter than* $\inf_\lambda i_\lambda(x_0)$*, the continuation method with initial condition of the shooting equation at* x_0 *converges,*

– *for length shorter than* $\inf_\lambda i_\lambda$ *the continuation method converges for every initial condition of the shooting equation.*

Remark 2.2. In the Riemannian case, the situation is neat. Completeness leads to existence of smooth normal minimizers, the domain of the exponential mapping is a sphere, and estimates of the injectivity radius are related to the curvature tensor. In general, such estimates are a difficult problem and a pragmatic point of view is to have numerical approximations [12].

3 The energy minimization problem in orbital transfer with low thrust

3.1 Preliminaries

Neglecting the mass variation and restricting to the coplanar case, the system is represented in Cartesian coordinates by

$$\ddot{q} = -\frac{q}{|q|^3} + u$$

where $q = (q_1, q_2)$ is the position and $x = (q, \dot{q}) \in \mathbf{R}^4$ is the state. We denote by $H_0(q, \dot{q}) = (1/2)\dot{q}^2 - 1/|q|$ the Hamiltonian of the free motion. We have the following first integrals:

– $C = q \wedge \dot{q}$ (momentum),

– $\mathrm{L} = -q/|q| + \dot{q} \wedge C$ (Laplace integral).

Proposition 3.1. *The domain* $\Sigma_e = \{(q, \dot{q}) \mid H < 0,\ C \neq 0\}$*, called the* elliptic domain*, is filled by elliptic orbits and to each orbit* (C, L) *corresponds a unique (oriented) ellipse.*

To represent the space of ellipses, one introduces the following geometric coordinates:

– the *semi-major axis* of the ellipse a, related to the *semi-latus rectum* P by the relation $a = P/\sqrt{1 - e^2}$,

– the argument of the pericenter θ,

– the *eccentricity* e, the *eccentricity vector* being $(e_x, e_y) = (e\cos\theta, e\sin\theta)$.

To represent the position of the satellite we use the *longitude* $l \in \mathbf{S}^1$, while $l \in \mathbf{R}$ takes into account the rotation number and is called the *cumulated longitude*. Observe that $e = 0$ corresponds to circular orbits. The control u can be decomposed into moving frames attached to the satellite, the two standard frames being

– the *radial-orthoradial* frame $\{F_r, F_{or}\}$ where $F_r = (q/|q|)\,\partial/\partial\dot{q}$,

– the *tangential-normal* frame $\{F_t, F_n\}$ where $F_t = (\dot{q}/|\dot{q}|)\,\partial/\partial\dot{q}$.

3.2 Averaging of periodic sub-Riemannian problems

Let X be an n-dimensional smooth manifold and let $F_i(l,x), i = 1,\dots,m$ be smooth vector fields parameterized by $l \in \mathbf{S}^1$ that set up a constant rank m distribution on X (see also Remark 3.2). Given a positive pulsation ω on $\mathbf{S}^1 \times X$ relating the time t and the angle l according to

$$\mathrm{d}l = \omega(l,x)\mathrm{d}t, \tag{3}$$

one defines a *periodic sub-Riemannian* problem as follows: Given two points x_0 and x_f on the manifold, minimize the $\mathrm{L}^2\mathrm{d}t$ control norm of trajectories connecting the two points and associated with the previous vector fields,

$$\frac{\mathrm{d}x}{\mathrm{d}l} = \sum_{i=1}^{m} u_i F_i(l,x), \quad u \in \mathbf{R}^m,$$

$$\min_{u(.)} \int_0^{t_f} |u|^2 \mathrm{d}t = \int_0^{l_f} |u|^2 \frac{\mathrm{d}l}{\omega(l,x)} \quad (\text{here } |u|^2 = \sum_{i=1}^{m} |u_i|^2).$$

The total angular length, $l_f > 0$ is fixed, implicitly defining t_f through (3).

Pontryagin maximum principle asserts that minimizing trajectories are projection of Hamiltonian curves on the cotangent bundle (extremals), $z = (x,p)$, such that

$$\frac{\mathrm{d}x}{\mathrm{d}l} = \frac{\partial H}{\partial p}(l,x,p,u), \qquad \frac{\mathrm{d}p}{\mathrm{d}l} = -\frac{\partial H}{\partial x}(l,x,p,u),$$

where

$$H(l,x,p,u) = p^0|u|^2 + \sum_{i=1}^{m} u_i H_i(l,x,p), \quad H_i = \langle p, F_i(l,x)\rangle, \quad i = 1,\dots,m,$$

is the Hamiltonian parameterized by $l \in \mathbf{S}^1$, $u \in \mathbf{R}^m$, and a non-positive constant p^0. We restrict the analysis to the normal case, $p^0 < 0$, and pass to affine coordinates in (p^0, p) setting $p^0 = -1/2$. Pontryagin maximization condition that, almost everywhere along an extremal,

$$H(l,z(l),u(l)) = \max_{v \in \mathbf{R}^m} H(l,z(l),v),$$

implies that the control is given by the dynamic feedback

$$u(l,z) = \omega(l,x)(H_1,\dots,H_m)(l,z), \tag{4}$$

and that z is an integral curve of the maximized Hamiltonian

$$H_n(l,z) = \frac{\omega(l,x)}{2} \sum_{i=1}^{m} H_i^2(l,z).$$

We are interested in the behaviour of solutions for large angular length, so we set $\varepsilon = 1/l_f$ as the small parameter and renormalize the problem in the following manner—typical of systems with two time scales.

In contrast to l which is the *fast time*, define the *slow time* $s = \varepsilon l$ in $[0,1]$, and renormalize variables on the cotangent bundle by

$$\widetilde{x} = x, \quad \widetilde{p} = p/\varepsilon.$$

Lemma 3.1. *In the renormalized variables,*

$$\frac{\mathrm{d}\widetilde{z}}{\mathrm{d}s} = \overrightarrow{H}_n(s/\varepsilon, \widetilde{z}). \tag{5}$$

Proof. Obvious since $H_n(l, x, \cdot)$ is quadratic in the adjoint state p. □

For fixed z, $H_n(\cdot, z)$ is a smooth function on $\mathbf{S}^1$ and can be expanded into its Fourier series. In particular, one can define its first coefficient or average,

$$H(z) = \frac{1}{2\pi} \int_0^{2\pi} H_n(l, z)\, \mathrm{d}l.$$

Since taking symplectic vector field and averaging readily commute, it is well known [2, 20] that H trajectories are good approximations of those of H_n as ε goes to zero.

Theorem 3.1. *Given any initial condition, the solution $\widetilde{z}_\varepsilon$ of (5) converges uniformly on $[0, 1]$ towards the solution $\overline{z}$ of the averaged Hamiltonian.*

Remark 3.1. The same rate of convergence holds for the cost which can be added as a new state in the augmented system. But as the integrand depends on the fast variable l through the pulsation ω, there is *a priori* no higher order approximation of the performance index [4, 15].

As for $H_n(s/\varepsilon, z)$ which converges to H in the large space of Schwartz distributions,[1] one can only expect weak convergence on the control u_ε of the original problem on $[0, 1/\varepsilon]$. We address two questions: first, can we describe the fast oscillating control by means of Fourier series with slowly varying coefficients and, secondly, what is the asymptotic behaviour of $\|u_\varepsilon\|_\infty$ when $\varepsilon \to 0$? The importance of such an estimate relies on the fact that one has in practice to estimate l_f so as to meet a given requirement on the L^∞-norm of the control.

We first note that the average system provides a sub-Riemannian approximation of the original one.

Proposition 3.2. *The averaged Hamiltonian is a nonnegative quadratic form in the adjoint. If constant, its rank is not less than m, and H can locally be written as a sum of squares, thus defining a sub-Riemannian (Riemannian if $k = n$) problem.*

Proof. Clearly, $H(x, \cdot)$ remains quadratic nonnegative in p by linearity and positivity of the integral and

$$\ker H(x, \cdot) = \bigcap_{l \in \mathbf{S}^1} \ker H_n(l, x, \cdot)$$

so that, if constant, the rank k is at least equal to m. In this case, the quadratic form can always be decomposed into a sum of k squares in a chart by taking the square root of the associated symmetric nonnegative matrix. □

Remark 3.2. (i) The increase in the rank is related to the generation of Lie brackets of the following system with drift: Set $\hat{x} = (l, x)$ and define

$$\hat{F}_0(\hat{x}) = \omega(\hat{x}) \frac{\partial}{\partial l}, \qquad \hat{F}_i(\hat{x}) = \omega(\hat{x}) F_i(\hat{x}), \quad i = 1, \ldots, m.$$

[1] Topological dual of the space of smooth compactly supported functions on the real line.

The fast oscillations (with respect to l) of the control in

$$\frac{\mathrm{d}\hat{x}}{\mathrm{d}t} = \hat{F}_0(\hat{x}) + \sum_{i=1}^{m} u_i \hat{F}_i(\hat{x})$$

generate new directions, namely

$$(\mathrm{ad}^j \hat{F}_0)\hat{F}_i, \quad j \geq 0,\ i = 1, \ldots, m,$$

a natural requirement being that the distribution $\{\hat{F}_0, \hat{F}_1, \ldots, \hat{F}_m\}$ on the augmented space $\mathbf{S}^1 \times X$ be bracket generating. This is equivalent to the bracket condition on $\mathbf{S}^1 \times X$ for the distribution $\{\partial/\partial l, F_1, \ldots, F_m\}$.
(ii) The assumption of rank constancy is sufficient to get a decomposition into a smooth sum of squares [3]. That the assumption is crucial is illustrated by the fact that it cannot be removed, even in the analytical category. Eigenvalues (and associated projectors) are indeed analytic functions on the set of matrices in the neighbourhoud of a simple (hence diagonalizable) endomorphism [22, Theorem II.5.16]. Avoiding semi-simple eigenvalues is necessary as is clear considering

$$\begin{bmatrix} x_1 & x_2 \\ x_2 & -x_1 \end{bmatrix}$$

whose eigenvalues are not differentiable at $(0, 0)$. But even in the simple symmetric nonnegative analytic case, existence of a differentiable square root matrix may fail as illustrated by

$$\begin{bmatrix} x_1^2 + x_2^2 & 0 \\ 0 & 1 \end{bmatrix}. \tag{6}$$

To get a positive result with non constant rank, one must actually restrict to the symmetric nonnegative case with analytic dependence on one real variable only. Eigenvalues and eigenvectors are then analytic on the real line [Ibid., Theorem II.6.1 and §II.6.2], and nonnegativeness ensures analyticity of square roots of the eigenvalues.
(iii) In the case of periodic sub-Riemannian systems, the loss of regularity may originate in averaging. The analytical distribution on $\mathbf{S}^1 \times \mathbf{R}^2$

$$F_1(l, x) = \sqrt{2}(x_1 \cos l + x_2 \sin l)\frac{\partial}{\partial x_1}, \quad F_2(l, x) = \frac{\partial}{\partial x_2}$$

has quadratic form

$$\begin{bmatrix} 2(x_1 \cos l + x_2 \sin l)^2 & 0 \\ 0 & 1 \end{bmatrix}$$

whose averaged is (6) which does not define an even differentiable sub-Riemannian system on $\mathbf{R}^2$.
(iv) A much stronger requirement is the existence of a change of coordinates on X (inducing a symplectic transformation on the cotangent) so that the averaged quadratic form be diagonal.

For a given $z \in T^*X$, let

$$u(l, z) = \sum_{k \in \mathbf{Z}} c_k(z) e_k(l), \quad e_k(l) = e^{ikl},$$

denote the Fourier series of the control (4). One has the following convergence result.

Proposition 3.3. *For any positive ε, the normal optimal control is*

$$u_\varepsilon(l) = \varepsilon \sum_{k\in\mathbf{Z}} c_k \circ \widetilde{z}_\varepsilon(\varepsilon l)\, e_k(l)$$

and the series converges pointwisely. Moreover, for any $k \in \mathbf{Z}$,

$$c_k \circ \widetilde{z}_\varepsilon \to c_k \circ \overline{z} \text{ uniformly on } [0,1] \text{ as } \varepsilon \to 0+$$

where the sub-Riemannian extremal $\overline{z}$ depends only on the boundary conditions x_0, x_f on X.

Proof. For $l \in [0, l_f]$,

$$\begin{aligned} u_\varepsilon(l) &= u(l, \widetilde{x}_\varepsilon(\varepsilon l), \varepsilon\widetilde{p}_\varepsilon(\varepsilon l)) \\ &= \varepsilon u(l, \widetilde{x}_\varepsilon(\varepsilon l), \widetilde{p}_\varepsilon(\varepsilon l)) \\ &= \varepsilon \sum_{k\in\mathbf{Z}} c_k(\widetilde{z}_\varepsilon(\varepsilon l))\, e_k(l) \end{aligned}$$

thanks to the pointwise convergence of the Fourier series at l for $z = \widetilde{z}_\varepsilon(l)$. For any $k \in \mathbf{Z}$,

$$c_k(z) = \frac{1}{2\pi}\int_0^{2\pi} u(l,z)\overline{e}_k(l)\mathrm{d}l$$

and the dependence on z is continuous since the integrand is bounded in a compact neighbourhood of the image of $\overline{z}$. □

Let us finally denote $\lambda(l,x)$ the biggest (positive) eigenvalue of the nonnegative quadratic form in p

$$|u(l,x,p)|^2 = \omega^2(l,x)\sum_{i=1}^{m} H_i^2(l,z) = 2\omega(l,x)H_n(l,z),$$

and define

$$\lambda(x) = \max_{l\in\mathbf{S}^1} \lambda(l,x).$$

As a supremum of continuous functions, $x \mapsto \lambda(x)$ is only lower semi-continous and we must assume the existence of a continous upper bound in the subsequent result.

Proposition 3.4. *Let σ be a continuous function such that σ^2 dominates λ in a neighbourhood of $\overline{x}$. Then*

$$\limsup_{\varepsilon\to 0+} \frac{\|u_\varepsilon\|_\infty}{\varepsilon} \le \|\sigma\circ\overline{x}\cdot|\overline{p}|\|_\infty.$$

Proof. On $[0, l_f]$, one has

$$\begin{aligned} |u_\varepsilon(l)|^2 &= \varepsilon^2 |u(l, \widetilde{z}_\varepsilon(\varepsilon l))|^2 \\ &\le \varepsilon^2 \sigma^2 \circ \widetilde{x}_\varepsilon(\varepsilon l)\cdot|\widetilde{p}_\varepsilon(\varepsilon l)|^2, \end{aligned}$$

so the result holds since the square root of the right hand side converges uniformly to $\sigma\circ\overline{x}\cdot|\overline{p}|$ as ε goes to zero by continuity of σ. □

3.3 Computations in Kepler case

Using the neat geometric coordinates of §3.1 on the three dimensional space of ellipses, we get

$$H_n(l,z) = \frac{\omega(l,x)}{2}(H_1^2+H_2^2)(l,z), \quad u(l,z) = \omega(l,x)(H_1,H_2)(l,z),$$
$$|u(l,z)|^2 = \omega^2(l,x)(H_1^2+H_2^2)(l,z), \tag{7}$$

with

$$\begin{aligned} F_1(l,x) &= \frac{P^2}{W^2}\left(\sin l\frac{\partial}{\partial e_x} - \cos l\frac{\partial}{\partial e_y}\right), \\ F_2(l,x) &= \frac{P^2}{W^2}\left(\frac{2P}{W}\frac{\partial}{\partial P}\right. \\ &\quad \left. +(\cos l + \frac{e_x+\cos l}{W})\frac{\partial}{\partial e_x} + (\sin l + \frac{e_y+\sin l}{W})\frac{\partial}{\partial e_y}\right), \end{aligned}$$

and

$$\omega(l,x) = \frac{W^2}{P^{3/2}}, \quad W = 1 + e_x\cos l + e_y \sin l.$$

Introducing *mean motion*, $n = a^{-3/2}$, and *true anomaly*, $\tau = l - \theta$, one gets

$$F_1(l,x) = \frac{P^2}{W^2}\left(-\frac{3en}{1-e^2}\frac{\partial}{\partial n} + \sin\tau\frac{\partial}{\partial e} - \cos\tau\frac{1}{e}\frac{\partial}{\partial\theta}\right), \tag{8}$$

$$\begin{aligned} F_2(l,x) &= \frac{P^2}{W^2}\left(-\frac{3Wn}{1-e^2}\frac{\partial}{\partial n} + (\cos\tau + \frac{e+\cos\tau}{W})\frac{\partial}{\partial e}\right. \\ &\quad \left. + (\sin\tau + \frac{\sin\tau}{W})\frac{1}{e}\frac{\partial}{\partial\theta}\right), \end{aligned} \tag{9}$$

with

$$W = 1 + e\cos\tau.$$

As a result, the computation of Fourier series of H_n (or u) are performed with respect to τ rather than l so, as θ only appears through τ,

$$H_n(l,z) = \sum_{k\in\mathbf{Z}} c_k(n,e,p)e_k(l-\theta) = \sum_{k\in\mathbf{Z}} c_k(z)e_k(l),$$

and coefficients verify

$$c_k(z) = c_k(n,e,p)\overline{e}_k(\theta).$$

Proposition 3.5. *The adjoint p_θ is a linear first integral of H.*

Proof. According to the previous remark, θ is cyclic in the averaged Hamiltonian. □

The remarkable feature of the set (n,e,θ) of coordinates is the following [17, 18, 7].

Proposition 3.6. *The averaged Hamiltonian is Riemannian and orthogonal in (n,e,θ) coordinates,*

$$H(z) = \frac{1}{2n^{5/3}}\left[9n^2p_n^2 + \frac{5}{2}(1-e^2)p_e^2 + \frac{5-4e^2}{2}\frac{p_\theta^2}{e^2}\right].$$

Fourier coefficients of the control are obviously obtained from (8-9), noting that

Lemma 3.2. *One has*

$$\frac{e+\cos\tau}{W} = -z - \frac{2\sqrt{1-e^2}}{e}\sum_{k\geq 1} z^k \cos k\tau, \quad \frac{\sin\tau}{W} = -\frac{2}{e}\sum_{k\geq 1} z^k \sin k\tau,$$

where $z = -e/(1+\sqrt{1-e^2})$ *is the only pole in the open unit disk of* $W = 1 + e\cos\tau$.

We finally provide a continuous upper bound of the eigenvalues of the quadratic form associated with the control norm, allowing us to estimate precisely $\|u_\varepsilon\|_\infty$ as $\varepsilon \to 0+$.

Proposition 3.7. *Eigenvalues of the quadratic form (7) are uniformly dominated by*

$$\sigma^2(n,e) = \frac{4(1-e^2)}{n^{2/3}}\left[\frac{(1+e)^2}{n^{4/3}} + 1\right] + \frac{e}{n^{2/3}}\left[e + \sqrt{1-e^2}\right].$$

Proof. Since we have a rank two distribution (8-9) of vector fields (parameterized by $l \in \mathbf{S}^1$) on the three-dimensional manifold X, a simple computation shows that the maximum eigenvalue is

$$\lambda(l,x) = \frac{\omega^2(l,x)}{2}\left[F_1^2 + F_2^2 + \sqrt{(F_1^2 - F_2^2)^2 + 4(F_1|F_2)^2}\right](l,x),$$

hence the result. □

The resulting estimate provided by Proposition 3.4 depends only on the geodesic connecting the two prescribed points on the manifold. Complete quadrature for these geodesics are computed in the next section.

3.4 Analysis of the averaged system

The main step in the analysis is to use further normalizations to obtain a geometric interpretation.

Proposition 3.8. *In the elliptic domain, we set*

$$r = \frac{2}{5}n^{5/6}, \quad \varphi = \arcsin e,$$

and the metric is isometric to

$$g = \mathrm{d}r^2 + \frac{r^2}{c^2}(\mathrm{d}\varphi^2 + G(\varphi)\mathrm{d}\theta^2)$$

with

$$c = \sqrt{2/5} \quad \textit{and} \quad G(\varphi) = \frac{5\sin^2\varphi}{1+4\cos^2\varphi}\cdot$$

Geometric interpretation. This normal form captures the main properties of the averaged orbital transfer. Indeed, we extract from g two Riemannian metrics in dimension two

$$g_1 = \mathrm{d}r^2 + r^2\mathrm{d}\psi^2$$

with $\psi = \varphi/c$ which is associated with orbital transfer where θ is kept fixed, and also

$$g_2 = \mathrm{d}\varphi^2 + G(\varphi)\mathrm{d}\theta^2$$

which represents the restriction to $r^2 = c^2$.

3.4.1 Analysis of $\mathbf{g_1}$

When p_θ vanishes, θ is constant. The corresponding extremals are geodesics of the Riemannian problem in dimension two defined by $\mathrm{d}\theta = 0$. We extend the elliptic domain to the *meridian half-planes* all isometric to

$$\Sigma_0 = \{n > 0,\ e \in]-1, +1[\}.$$

In polar coordinates (r, ψ), Σ_0 is defined by $\{r > 0, \psi \in]-\pi/(2c), \pi/(2c)[\}$. This extension allows to go through the singularity corresponding to circular orbits. Geometrically, this describes transfers where the angle of the pericenter is kept fixed and $p_\theta = 0$ corresponds to the transversality condition. Such a policy is clearly associated with steering the system towards circular orbits where the angle θ of the pericenter is not prescribed. An important physical subcase is the geostationary final orbit.

In the domain Σ_0, the metric $g_1 = \mathrm{d}r^2 + r^2\mathrm{d}\psi^2$ is a polar metric isometric to the flat metric $\mathrm{d}x^2 + \mathrm{d}z^2$ if we set $x = r\sin\psi$ and $z = r\cos\psi$.
We deduce the following proposition.

Proposition 3.9. *The extremals of the averaged coplanar transfer in Σ_0 are straight lines in suitable coordinates, namely*

$$x = \frac{2^{3/2}}{5}n^{5/6}\sin(c^{-1}\arcsin e), \quad z = \frac{2^{3/2}}{5}n^{5/6}\cos(c^{-1}\arcsin e)$$

with $c = \sqrt{2/5}$. Since $c < 1$, the domain is not convex and the metric g_1 is not complete.

Proof. The axis $e_x = 0$ corresponds to circular orbits. Among the extremals, we have two types (see Fig. 1): complete curves of type 1, and non-complete curves of type 2 that meet the boundary of the domain. The domain is not geodesically convex and in subdomain II, the existence theorem fails. For each initial condition, there exists a separatrix S which corresponds to a segment line in the orbital coordinates which is meeting $n = 0$ in finite time. Its length gives the bound for a sphere to be compact. □

In order to complete the analysis of g and to understand the role of g_2, we present now the integration algorithm.

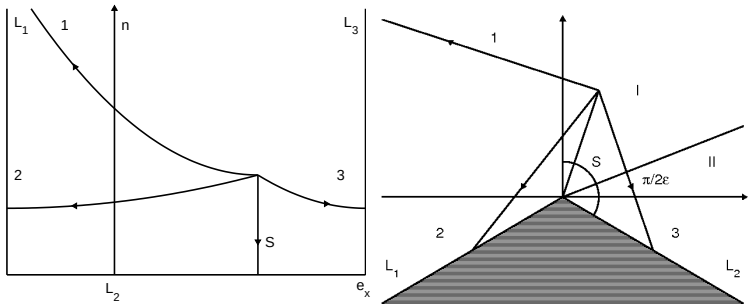

Figure 1: Geodesics of the metric g_1 in (n, e_x) and flat coordinates.

3.4.2 Integrability of the extremal flow

The integrability property is a consequence of the normal form only,

$$g = \mathrm{d}r^2 + r^2(\mathrm{d}\varphi^2 + G(\varphi)\mathrm{d}\theta^2),$$

and the associated Hamiltonian is decomposed into

$$H = \frac{1}{2}p_r^2 + \frac{1}{r^2}H', \quad H' = \frac{1}{2}(p_\varphi^2 + \frac{p_\theta^2}{G(\varphi)}).$$

Lemma 3.3. *The Hamiltonian vector field $\overrightarrow{H}$ admits three independent first integrals in involution, H, H', p_θ, and is Liouville integrable.*

To get a complete parameterization, we proceed as follows. We use the (n, e, θ) coordinates and write

$$H = \frac{1}{4n^{5/3}}[18n^2p_n^2 + H'']$$

with

$$H'' = 5(1-e^2)p_e^2 + \frac{5-4e^2}{e^2}p_\theta^2.$$

Lemma 3.4. *Let $s = n^{5/3}$ then $s(t)$ is a polynomial of degree 2, $s(t) = c_1t^2 + \dot{s}(0)t + s(0)$ with $s(0) = n^{5/3}(0)$, $\dot{s}(0) = 15n(0)p_n(0)$ and $c_1 = 25H/2$.*

Lemma 3.5. *Let $\mathrm{d}T = \mathrm{d}t/4n^{5/3}$. If $H''(0) \neq 0$, then*

$$T(t) = \frac{1}{2\sqrt{|\Delta|}}[\arctan L(s)]_0^t$$

where $L(t) = (2at + b)/\sqrt{|\Delta|}$, $a = c_1$, $b = \dot{s}(0)$ and $\Delta = -25H''(0)/2$ is the discriminant of $s(t)$.

This allows to make the integration. Indeed if $H'' = 0$, $p_e = p_\theta = 0$ and the trajectories are straight lines (the line S in Fig. 1). Otherwise, we observe that $n^{5/3}(t)$ is known and depends only upon $n(0)$, $p_n(0)$ and H which can be fixed to $1/2$ by parameterizing by arc length. Hence, it is sufficient to integrate the flow associated with H'' using the parameter $\mathrm{d}T = \frac{\mathrm{d}t}{4n^{5/3}}$ where T is given by

the previous lemma. Let $H'' = c_3^2$ and $p_\theta = c_2$. Using $p_e = \dot{e}/10(1-e^2)$, we obtain

$$\dot{e}^2 = \frac{20(1-e^2)}{e^2}[c_3 e^2 - (5-4e^2)c_2^2].$$

To integrate, we set $w = 1-e^2$ for $e \in]0,1[$, so the equation takes the form

$$\frac{\mathrm{d}w}{\mathrm{d}T} = Q(w)$$

where

$$Q(w) = 80w[(c_3^2 - c_2^2) - (c_3^2 + 4c_2^2)w]$$

with positive discriminant. Hence the solution is

$$w = \frac{1}{2}\frac{c_3^2 - c_2^2}{c_3^2 + 4c_2^2}\left[1 + \sin(\frac{4}{\sqrt{5}}\sqrt{c_3^2 + 4c_2^2})T + K\right],$$

K being a constant. We deduce that

$$\theta(T) = \theta(0) + 2c_2 \int_0^T \frac{1+4w(s)}{1-w(s)}\mathrm{d}s$$

where $\theta(0)$ can be set to 0 by symmetry. To conclude, we must integrate $(1+4w(s))/(1-w(s))$ with $w = K_1(1+\sin x)$ and $x = (4s/\sqrt{5})\sqrt{c_3^2+4c_2^2} + K$. Therefore, we must evaluate an integral of the form

$$\int \frac{A + B\sin x}{C + D\sin x}\mathrm{d}x.$$

More precisely, the formula is

$$\int \frac{A + B\sin x}{C + D\sin x}\mathrm{d}x = \frac{B}{D}x + AD - BC\int \frac{\mathrm{d}x}{C + D\sin x}$$

with

$$\int \frac{\mathrm{d}x}{C + D\sin x} = \frac{2}{\sqrt{C^2 - D^2}}\arctan\left(\frac{C\tan(x/2) + D}{\sqrt{C^2 - D^2}}\right)$$

and $C^2 - D^2 > 0$. The previous lemmas and computations give

Proposition 3.10. *For $H'' \neq 0$, the solutions of $\overrightarrow{H}$ can be computed using elementary functions and*

$$\begin{aligned}
n(t) &= \left[\frac{25}{2}Ht^2 + 15n(0)p_n(0)t + n^{5/3}(0)\right]^{3/5}, \\
e(t) &= \sqrt{1 - K_1(1+\sin K_2(t))}, \\
\theta(t) &= \theta(0) + \frac{p_\theta}{2|p_\theta|}K_3\left[-4x + \frac{10}{K_3}\arctan\frac{(1-K_1)\tan(x/2) - K_1}{K_3}\right]_K^{K_2(t)},
\end{aligned}$$

with

$$K = \arcsin\left(\frac{1-e(0)^2}{K_1} - 1\right), \quad K_1 = \frac{1}{2}\frac{H''(0) - p_\theta^2}{H''(0) + 4p_\theta^2},$$

$$K_2(t) = \frac{4}{\sqrt{5}}\left(T(t)\sqrt{H''(0) + 4p_\theta^2} + K\right), \quad K_3 = \sqrt{\frac{5p_\theta^2}{H''(0) + 4p_\theta^2}}.$$

For $H'' = 0$, they are straight lines.

Remark 3.3. The above formulas give the complete solution of the associated Hamilton-Jacobi Equation.

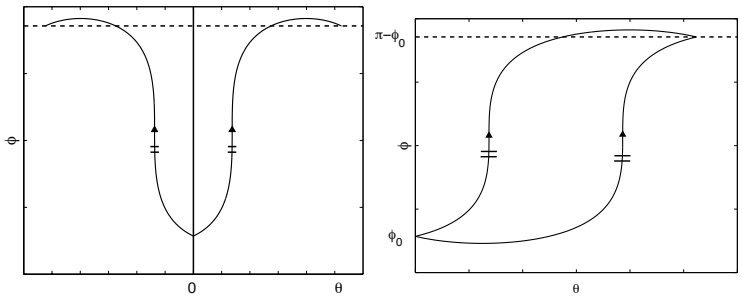

Figure 2: Action of the symmetry group on the extremals.

3.4.3 Geometric properties of $\mathbf{g_2}$

The previous integration algorithm shows that the extremals of this metric describe the evolution of the angular variables θ and φ parameterized by $\mathrm{d}T = \mathrm{d}t/r(t)^2$ where $r(t)^2$ is a second order polynomial whose coefficients depend only upon the energy level H fixed to $1/2$, $r(0)$ and $p_r(0)$. We now give some basic properties of g_2.

Lemma 3.6. *The metric g_2 can be extended to an analytic metric on the whole sphere $\mathbf{S}^2$, where θ and φ are spherical coordinates with two polar singularities at $\varphi = 0$ or π corresponding to $e = 0$, whereas the equator corresponds to $e = 1$; θ is an angle of revolution. The meridians are projections on $\mathbf{S}^2$ of the extremals of g_1.*

Lemma 3.7. *The two transformations $(\varphi, \theta) \mapsto (\varphi, -\theta)$ and $(\varphi, \theta) \mapsto (\pi - \varphi, \theta)$ are isometry of g_2. This induces the following symmetries for the extremal flow:*

- *if $p_\theta \mapsto -p_\theta$ then we have two extremals of same length symmetric with respect to the meridian $\theta = 0$,*
- *if $p_\varphi \mapsto -p_\varphi$ then we have two extremals of same length intersecting on the antipodal parallel, $\varphi = \pi - \varphi(0)$.*

Such properties (illustrated on Fig. 3.4.3) are shared by the following one-parameter family of metrics.

Metrics induced by the flat metric on oblate ellipsoid of revolution. We consider the flat metric of $\mathbf{R}^3$, $g = \mathrm{d}x^2 + \mathrm{d}y^2 + \mathrm{d}z^2$, restricted to the ellipsoid defined by

$$x = \sin\varphi\cos\theta,\ y = \sin\varphi\sin\theta,\ z = \mu\cos\varphi$$

where $\mu \in]0, 1[$. A simple computation leads to

$$E_\mu(\varphi)\mathrm{d}\varphi^2 + \sin^2\varphi\,\mathrm{d}\theta^2$$

for the restricted metric, where $E_\mu(\varphi) = \mu^2 + (1-\mu^2)\cos^2\varphi$, and we can write

$$g_2 = \frac{1}{E_\mu(\varphi)}(E_\mu(\varphi)\mathrm{d}\varphi^2 + \sin^2\varphi\,\mathrm{d}\theta^2)$$

where $\mu = 1/\sqrt{5}$. We deduce the following lemma.

Lemma 3.8. *The metric g_2 is conformal to the flat metric restricted to an oblate ellipsoid of revolution with parameter $\mu = 1/\sqrt{5}$.*

3.4.4 A global optimality result with application to orbital transfer

In this section, we consider an analytic metric on $\mathbf{R}_+ \times \mathbf{S}^2$

$$g = \mathrm{d}r^2 + (\mathrm{d}\varphi^2 + G(\varphi)\mathrm{d}\theta^2)$$

and let H be the associated Hamiltonian. We fix the parameterization to arc length by restricting to the level set $H = 1/2$. Let x_1, x_2 be two extremal curves starting from the same initial point x_0 and intersecting at some positive $\bar{t}$. We get the relations

$$r_1(\bar{t}) = r_2(\bar{t}), \quad \varphi_1(\bar{t}) = \varphi_2(\bar{t}), \quad \theta_1(\bar{t}) = \theta_2(\bar{t}),$$

and from Lemma 3.4, we deduce that

Lemma 3.9. *Both extremals x_1 and x_2 share the same $p_r(0)$ and for each t, $r_1(t) = r_2(t)$.*

If we consider now the integral curves of H' where $H = (1/2)p_r^2 + H'/r^2$ on the fixed induced level and parameterize these curves using $\mathrm{d}T = \mathrm{d}t/r^2$, we deduce the following characterization.

Proposition 3.11. *The following conditions are necessary and sufficient to characterize extremals of $H' \neq 0$ intersecting with same length*

$$\varphi_1(\overline{T}) = \varphi_2(\overline{T}) \quad \textit{and} \quad \theta_1(\overline{T}) = \theta_2(\overline{T})$$

together with the compatibility condition

$$\overline{T} = \int_0^{\bar{t}} \frac{\mathrm{d}t}{r^2(t)} = \left[\frac{2}{\sqrt{\Delta}} \arctan L(t) \right]_{t=0}^{\bar{t}}.$$

Theorem 3.2. *A necessary global optimality condition for an analytic metric on $\mathbf{R}_+ \times \mathbf{S}^1$ normalized to*

$$g = \mathrm{d}r^2 + r^2(\mathrm{d}\varphi^2 + G(\varphi)\mathrm{d}\theta^2)$$

is that the injectivity radius be greater than or equal to π on the sphere $r = 1$, the bound being reached by the flat metric in spherical coordinates.

Proof. We observe that in the flat case, the compatibility condition cannot be satisfied. Moreover, the injectivity radius on $\mathbf{S}^2$ is π corresponding to the half-length of a great circle. For the analytic metric on $\mathbf{S}^2$ under consideration, the injectivity radius is the length of the conjugate point at minimum distance or the half-length of a closed geodesic [16]. The conjugate point is, in addition, a limit point of the separating line. Hence, if the injectivity radius is smaller than π, we have two minimizers for the restriction of the metric on $\mathbf{S}^2$ which intersects with a length smaller than π. We shall show that it corresponds to a projection of two extremals x_1 and x_2 which intersect with same length.

For such extremals $r(0) = 1$, we set $p_r(0) = \varepsilon$, $H = 1/2$ and we get

$$2H' = p_\varphi^2(0) + \frac{p_\theta^2(0)}{G(\varphi(0))} = \lambda^2(\varepsilon), \quad \lambda(\varepsilon) = \sqrt{1-\varepsilon^2}.$$

If t_1 is the injectivity radius on the level set $H' = 1/2$, for $H' = \lambda^2(\varepsilon)/2$ and $p_r(0) = \varepsilon$, it is rescaled to $T_1 = t_1/\lambda(\varepsilon)$. The compatibility relation for $\overline{T} = T_1$ then gives

$$T_1 = \arctan \frac{\bar{t} + \varepsilon}{\lambda(\varepsilon)} - \arctan \frac{\varepsilon}{\lambda(\varepsilon)}.$$

Clearly, the maximum of the right member is π, taking $\varepsilon < 0$, $|\varepsilon| \to 1$. Hence, it can be satisfied since $t_1 < \pi$. The flat case shows that it is the sharpest bound. □

By homogeneity, we deduce the following corollary.

Corollary 3.1. *If the metric is normalized to* $\mathrm{d}r^2 + (r^2/c^2)(\mathrm{d}\varphi^2 + G(\varphi)\mathrm{d}\theta^2)$, *then the bound for the injectivity radius on* $r^2 = c^2$ *is* $c\pi$.

3.4.5 Riemannian curvature and injectivity radius in orbital transfer

Using standard formulæ from Riemannian geometry [16], we have the following proposition.

Proposition 3.12. *Let* g *be a smooth metric of the form* $\mathrm{d}r^2 + r^2(\mathrm{d}\varphi^2 + G(\varphi)\mathrm{d}\theta^2)$. *The only non-zero component of the Riemann tensor is*

$$R_{2323} = r^2 \left[-\frac{G''(\varphi)}{2} - G(\varphi) + \frac{G'(\varphi)^2}{4G(\varphi)} \right]$$

which takes the form $R_{2323} = -r^2 F(F'' + F)$ *if we set* $G(\varphi) = F^2(\varphi)$. *We have therefore* $R_{2323} = 0$ *if and only if* $F(\varphi) = A\sin(\varphi + \varphi_0)$ *which is induced by the flat case in spherical coordinates.*

Hence, the main non-zero sectional curvature of the metric is

$$K = \frac{R_{2323}}{|\frac{\partial}{\partial\theta} \wedge \frac{\partial}{\partial\varphi}|^2}$$

and computing this term in the case of orbital transfer, we get:

Lemma 3.10. *The sectional curvature in the plane* (φ, θ) *is given by*

$$K = \frac{(1 - 24\cos^2\varphi - 16\cos^4\varphi)}{r^2(1 + 4\cos^2\varphi)^2}$$

and $K \to 0$ *as* $r \to +\infty$.

Proposition 3.13. *The Gauss curvature of the metric of* $g_2 = \mathrm{d}\varphi^2 + G(\varphi)\mathrm{d}\theta^2$ *with* $G(\varphi) = (\sin^2\varphi)/(1 + 4\cos^2\varphi)$ *is*

$$K = \frac{5(1 - 8\cos^2\varphi)}{(1 + 4\cos^2\varphi)^2}.$$

Theorem 3.3. *The Gauss curvature of g_2 is negative near the poles and maximum at the equator. The injectivity radius is $\pi/\sqrt{5}$ and is reached by the shortest conjugate point along the equator.*

Proof. Clearly K is maximum and equal to five along the equator which is an extremal solution. Hence a direct computation gives that the shortest conjugate point is on the equator with length $\pi/\sqrt{5}$. It corresponds to the injectivity radius if the half-length of a shortest periodic extremal is greater than $\pi/\sqrt{5}$. Simple closed extremals are computed in [8] using the integrability property and a simple reasoning gives that the shortest corresponds to meridians whose length is 2π. Hence the result is proved. □

Corollary 3.2. *Since $\pi/\sqrt{5} < \pi\sqrt{2/5}$, the necessary optimality condition of Theorem 3.3 is not satisfied in orbital transfer for the extension of the metric to $\mathbf{R}^+ \times \mathbf{S}^2$.*

3.4.6 Cut locus on $\mathbf{S}^2$ and global optimality results in orbital transfer

From the previous section, the computation of the injectivity radius for the metric on $\mathbf{S}^2$ is not sufficient to conclude about global optimality. A more complete analysis is necessary to evaluate the cut locus. This analysis requires numerical simulations. The main results are [8, 11]:

Proposition 3.14. *For the metric g_2 on $\mathbf{S}^2$, they are exactly five simple closed geodesics modulo rotations around the poles, the shortest being meridians with length 2π, the longest the equator with length $2\pi\sqrt{5}$.*

Theorem 3.4. *Except for poles, the conjugate locus is a deformation of a standard astroid with axial symmetry and two cusps located on the antipodal parallel. With the exception of poles, the cut locus is a simple segment, located on the antipodal parallel, with axial symmetry, and whose extremities are cusps points of the conjugate locus. For a pole, the cut locus is reduced to the antipodal pole.*

Proof. The proof is made by direct analysis of the extremal curves. The main problem is to prove that the separating line is given by points on the antipodal parallel where, because of the isometry $\varphi \to \pi - \varphi$, two extremals curves with same length intersect. This property cannot occur before. The results are represented Fig. 3. □

Geometric interpretation and comments. The metric is conformal to the restriction of the flat metric to an oblate ellipsoid of revolution. For such a metric, the cut locus is known since Jacobi and is similar to the one represented on Fig. 3. It is a remarkable property that there is no bifurcation of the cut locus when the metric is deformed by the factor $E_\mu(\varphi)$ In orbital transfer for instance, the Gauss curvature is not positive. On $\mathbf{S}^2$, relations between the conjugate and cut loci allow to deduce the cut locus from the conjugate locus.[2] The conjugate locus can also easily be computed using the code [12]. It can also be deduced by inspecting the extremal flow only, the conjugate locus being an envelope.

[2]For instance, a domain bounded by two intersecting minimizing curves must contain a conjugate point.

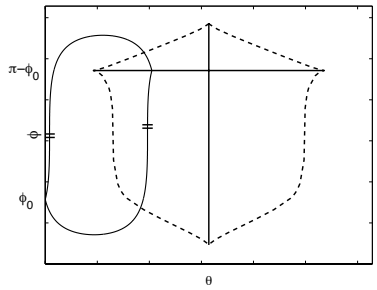

Figure 3: Conjugate and cut loci in averaged orbital transfer.

Finally, we observe that in order to have intersecting minimizers, we must cross the equator $\varphi = \pi$, that is $e = 1$. The same is true for conjugate points. Hence we deduce

Theorem 3.5. *Conjugate loci and separating lines of the averaged Kepler metric are always empty in the spaces of ellipses where* $e \in [0, 1[$.

3.5 The averaged system in the tangential case

An interesting question is to analyze if the averaged system in the *tangential case* where the control is oriented along F_t retains similar properties [10]. The first step is to compute the corresponding averaged system.

Proposition 3.15. *If the control is oriented along* F_t *only, the averaged Hamiltonian associated with energy minimization is*

$$H_t = \frac{1}{2n^{5/3}} \left[9n^2 p_n^2 + \frac{4(1-e^2)^{3/2}}{1+\sqrt{1-e^2}} p_e^2 + \frac{4(1-e^2)}{1+\sqrt{1-e^2}} \frac{p_\theta^2}{e^2} \right]$$

and corresponds to the Riemannian metric

$$g_t = \frac{\mathrm{d}n^2}{9n^{1/3}} + \frac{n^{5/3}}{4} \left[\frac{1+\sqrt{1-e^2}}{(1-e^2)^{3/2}} \mathrm{d}e^2 + \frac{1+\sqrt{1-e^2}}{(1-e^2)} e^2 \mathrm{d}\theta^2 \right]$$

where (n, e, θ) *remain orthogonal coordinates.*

3.5.1 Construction of the normal form

We proceed as in Section 3.4 and set

$$r = \frac{2}{5} n^{5/6}, \quad e = \sin\varphi \sqrt{1+\cos^2\varphi}\,.$$

The metric becomes

$$g_t = \mathrm{d}r^2 + \frac{r^2}{c^2}(\mathrm{d}\varphi^2 + G(\varphi)\mathrm{d}\theta^2), \quad c = \frac{2}{5} < 1,$$

and

$$G(\varphi) = \sin^2\varphi \left(\frac{1 - (1/2)\sin^2\varphi}{1 - \sin^2\varphi} \right)^2 .$$

Hence the normal form is similar to the full control case. As before, we introduce the metrics

$$g_1 = \mathrm{d}r^2 + r^2\mathrm{d}\psi^2, \quad \psi = \varphi/c,$$

and

$$g_2 = \mathrm{d}\varphi^2 + G(\varphi)\mathrm{d}\theta^2.$$

The main difference with the full control case will concern the singularities of the function G.

3.5.2 Metrics $\mathbf{g_1}$ and $\mathbf{g_2}$

The metric g_1 corresponds again to transfer to circular orbits and is the polar form of the flat metric $\mathrm{d}x^2 + \mathrm{d}z^2$, if $x = r\sin\psi$ and $z = r\cos\psi$.

The normal form reveals the same homogeneity property between the full control and the tangential case, so the metric g_2 can be used to make a similar optimality analysis, evaluating the conjugate and cut locus. But the metric g_2 cannot be interpreted as a smooth metric on $\mathbf{S}^2$. This can be seen by computing the Gauss curvature.

Proposition 3.16. *The Gauss curvature of g_2 is given by*

$$K = \frac{(3+\cos^2\varphi)(\cos^2\varphi - 2)}{(1+\cos^2\varphi)\cos^2\varphi}.$$

In particular $K \to -\infty$ when $\varphi \to \pi/2$, and since $K < 0$, the conjugate locus of any point is empty.

Nevertheless, the extremals can be smoothly extended through the singular boundary of the domain, the equator $\varphi = \pi/2$.

3.5.3 Integration of the extremal flow

The algorithm based on the normal form is similar to the bi-input case, but we compare the respective transcendence. The Hamiltonian is written

$$H = \frac{1}{4n^{5/3}}[18n^2p_n^2 + H'']$$

where H'' now takes the form

$$H'' = \frac{8(1-e^2)^{3/2}}{1+\sqrt{1-e^2}}p_e^2 + \frac{8(1-e^2)}{1+\sqrt{1-e^2}}\frac{p_\theta^2}{e^2}.$$

We set $H'' = c_3^2$, $p_\theta = c_2$, and from

$$p_e = 4n^{5/3}\,\frac{(1+\sqrt{1-e^2})e}{16(1-e^2)^{3/2}}$$

we obtain

$$\left(\frac{\mathrm{d}w}{\mathrm{d}T}\right)^2 = \frac{Q(w)}{(1+w)^2}$$

where $w = \sqrt{1-e^2}$, T is as in the bi-input case, and Q is the fourth-order polynomial

$$Q(w) = 32w[c_3^2(1-w^2)(1+w) - 8c_2^2w^2].$$

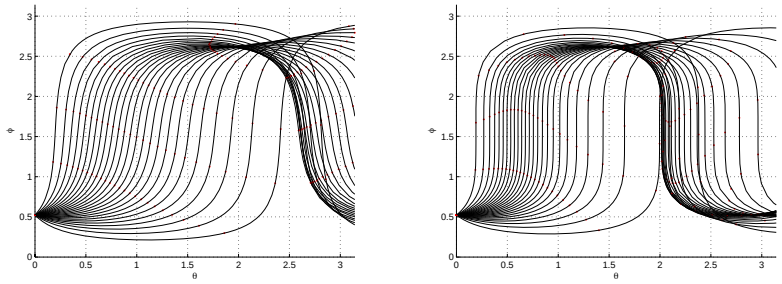

Figure 4: Extremal flow of g_2 in the full control and tangential cases, in the (φ, θ) coordinates, starting from $\varphi = \pi/6$.

Hence, the integration requires the computation of the elliptic integral

$$\int \frac{\mathrm{d}w(1+w)}{\sqrt{Q(w)}}$$

which has an additional complexity. It is related to the pole of order 2 of the metric at the equator. See [9] for both aspects.

3.5.4 Conclusion in both cases

The previous analysis shows that the full control case and the tangential one admit a uniform representation in coordinates (θ, φ). In particular, it allows to make a continuation between the respective Hamiltonians, i.e., between the respective functions G. A correction has to be made between orbit elements e which are respectively defined by

$$e = \sin\varphi \quad \text{versus} \quad e = \sin\varphi\sqrt{1+\cos^2\varphi}.$$

The flows in the two cases are presented on Fig. 4 and reveal the similar structure. The conjugate locus is reached after having crossed the equator. On Fig. 5 and 6 we present a first continuation result, in the tangential case, showing the convergence of the method from the averaged to the non averaged trajectory for specific transfer orbits.

3.6 Conjugate and cut loci on a two-sphere of revolution

The problem of computing the conjugate and cut loci in orbital transfer is connected to a very old geometric problem which goes back to Jacobi and is briefly introduced next.

Definition 3.1. The two-sphere $\mathbf{S}^2$ endowed with a smooth metric of the form $\mathrm{d}\varphi^2 + G(\varphi)\mathrm{d}\theta^2$ in spherical coordinates is called *two-sphere of revolution*.

Many of them can be realized as Riemannian surfaces of revolution embedded in $\mathbf{R}^3$ by rotating on a smooth curve homeomorphic to a half-circle. The classical examples are the following:

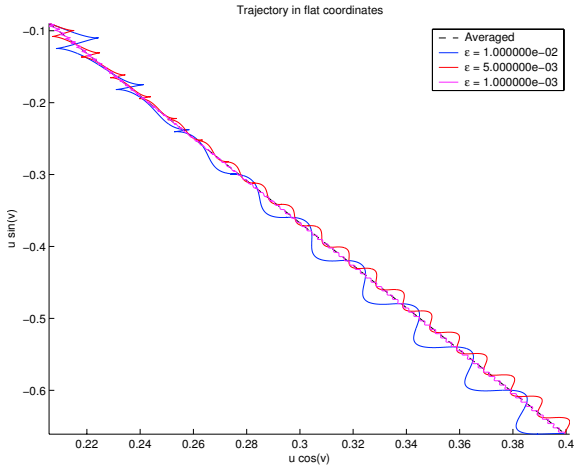

Figure 5: Computation by continuation of the non-averaged solution. The averaged trajectories are clearly nice approximations of the optimal ones of the original system. Hence, convergence of the underlying shooting method to compute the non-averaged minimizing trajectory is easily obtained.

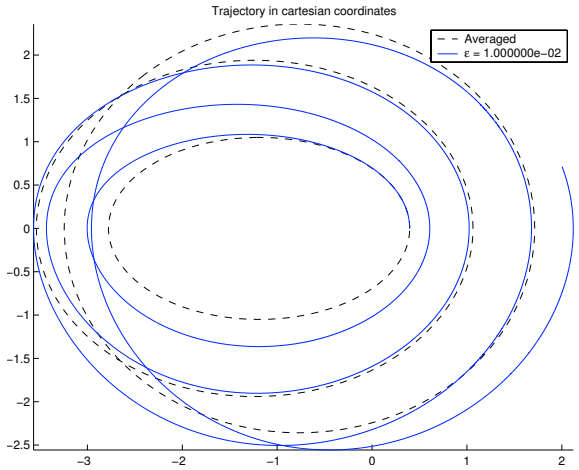

Figure 6: Trajectory of a non-averaged solution for $\varepsilon = 1e{-}2$ with $(e(0), n(0)) = (7.5e{-}1, 5e{-}1)$ and $(e(t_f), n(t_f)) = (5e{-}2, 3e{-}1)$. Dashed ellipses are averaged ellipses and provide a good approximation of the motion.

- *Round sphere* $\mathbf{S}^2$. It is constructed restricting the Euclidian metric to $\mathbf{S}^2$ and given by $\mathrm{d}\varphi^2 + \sin^2(\varphi)\mathrm{d}\theta^2$.
- *Oblate ellipsoid of revolution* $O(\mu)$. If we restrict the Euclidian metric to the surface

$$x = \sin\varphi\cos\theta, \quad y = \sin\varphi\sin\theta, \quad z = \mu\cos\varphi,$$

with $\mu < 1$, the metric is $(1 - (1-\mu^2)\sin^2\varphi)\mathrm{d}\varphi^2 + \sin^2(\varphi)\mathrm{d}\theta^2$ which can be set in the form $\mathrm{d}\varphi^2 + G(\varphi)\mathrm{d}\theta^2$ using a quadrature.

We recall some basic properties on the ellipsoid of revolution.

Proposition 3.17. *On an oblate ellipsoid of revolution,*

- *the Gauss curvature is monotone increasing from the North pole to the equator,*
- *the cut locus of a point which is not a pole is a subarc of the antipodal parallel,*
- *the conjugate locus of a point which is not a pole has a standard astroid shape with four cusps.*

The simple structure of the cut locus is a consequence of [30].

Theorem 3.6. *Let* $\mathrm{d}\varphi^2 + G(\varphi)\mathrm{d}\theta^2$ *be a metric on a two-sphere of revolution. We assume:*

- *The transformation* $\varphi \longrightarrow \pi - \varphi$ *is an isometry* i.e. $G(\pi - \varphi) = G(\varphi)$,
- *The Gauss curvature* K *is monotone non decreasing along a meridian from the North pole to the equator.*

Then, the cut locus of a point not a pole is a simple branch located on the antipodal parallel.

Application. Let g_λ be the family of analytic metrics on $\mathbf{S}^2$ defined by

$$g_\lambda = \mathrm{d}\varphi^2 + G_\lambda(\varphi)\mathrm{d}\theta^2, \quad G_\lambda(\varphi) = \frac{(1+\lambda)^2 \sin^2\varphi}{(1+\lambda\cos^2\varphi)}, \quad \lambda \geq 0.$$

The Gauss curvature is given by

$$K_\lambda = -\frac{1}{\sqrt{G}}\frac{\partial^2\sqrt{G}}{\partial^2\varphi} = \frac{(1+\lambda)(1-2\lambda\cos^2\varphi)}{(1+\lambda\cos^2\varphi)^2}.$$

Hence if $0 < \lambda \leq 2$, then K_λ is monotone non decreasing from the North pole to the equator and the previous theorem asserts that the one parameter family has a cut locus reduced to a simple branch for $\lambda \in]0, 2]$.

If $\lambda > 2$ the Gaussian curvature K_λ is not monotone and the result cannot be applied. In particular the orbit transfer with full control corresponds to $\lambda = 4$, while at the limit case $\lambda = +\infty$ a singularity appears. The Riemannian metric has a pole at the equator, the situation being similar to the one occuring when the thrust is only tangential. Hence Theorem 3.6 has to be refined to deal with such situations. The final result is coming from [9].

We consider a metric of the form $g = \varphi^2 + G(\varphi)\mathrm{d}\theta^2$ where G' is non zero on $]0, \frac{\pi}{2}[$ and $G(\pi - \varphi) = G(\varphi)$.

Definition 3.2. The *first return mapping* to the equator is the map

$$\Delta\theta : p_\theta \in]0, \sqrt{G}(\pi/2)[\mapsto \Delta\theta(p_\theta)$$

that is the θ-variation of the extremal parameterized by arc length and associated with the adjoint vector component p_θ. The extremal flow is called *tame* if the first return mapping is monotone non-increasing for $p_\theta \in]0, \sqrt{G}(\pi/2)[$.

Theorem 3.7. *In the tame case, the cut locus of a point different from a pole is a subset of the antipodal parallel. If moreover* $\Delta\theta'(p_\theta) < 0 < \Delta\theta''(p_\theta)$ *on* $]0, \sqrt{G}(\pi/2)[$*, then the conjugate locus of such a point has exactly four cusps.*

Remark 3.4. This result can be extended to the singular case where the metric has poles at the equator.

4 Energy minimization in the Earth-Moon space mission with low thrust

4.1 The N-body problem

In this section, we follow mainly [24] (see also [26] and [31]). Consider N point masses $m_1, \ldots, m_N$ moving in a Galilean reference system $\mathbf{R}^3$ where the only forces acting are their mutual attractions. If $q = (q_1, \ldots, q_N) \in \mathbf{R}^{3N}$ is the state and $p = (p_1, \ldots, p_N)$ is the momentum vector, the equations of motion are

$$\dot{q} = \frac{\partial H}{\partial p}\,, \quad \dot{p} = -\frac{\partial H}{\partial q}$$

where the Hamiltonian is

$$H = \sum_{i=1}^{N} \frac{|p_i|^2}{2m_i} - U, \quad U(q) = \sum_{1 \le i < j \le N} \frac{G m_i m_j}{|q_i - q_j|}.$$

A subcase is the coplanar situation where the N masses are in a plane $\mathbf{R}^2$. In this case the Galilean reference frame can be replaced by a rotating frame defined by

$$K = \begin{bmatrix} 0 & 1 \\ -1 & 0 \end{bmatrix}, \quad \exp(\omega t K) = \begin{bmatrix} \cos\omega t & \sin\omega t \\ -\sin\omega t & \cos\omega t \end{bmatrix},$$

and introducing a set of coordinates which uniformly rotates with frequency ω, one defines the symplectic transformation

$$u_i = \exp(\omega t K) q_i, \quad v_i = \exp(\omega t K).$$

A standard computation gives the Hamiltonian of the N-body problem in rotating coordinates,

$$H = \sum_{i=1}^{N} \frac{|v|^2}{2m_i} - \sum_{i=1}^{N} w^t u_i K v_i - \sum_{1 \le i < j \le N} \frac{G m_i m_j}{|q_i - q_j|}.$$

In particular, the Kepler problem in rotating coordinates up to a normalization has the following Hamiltonian

$$H = \frac{|p|^2}{2} - {}^t q K p - \frac{1}{|q|}.$$

4.2 The circular restricted 3-body problem in Jacobi coordinates

The following representation of the Earth-Moon problem fits in the so-called *circular restricted 3-body problem*. In the rotating frame, the Earth which is the biggest primary planet with mass $1-\mu$ is located at $(-\mu, 0)$ while the Moon with mass μ is located at $(1-\mu, 0)$ (the small parameter being $\mu \simeq 1.2153e-2$). We note $z = x + iy$ the position of the spacecraft, and ρ_1, ρ_2 the distances to the primaries,

$$\begin{aligned} \rho_1 &= \sqrt{(x+\mu)^2 + y^2}, \\ \rho_2 &= \sqrt{(x-1+\mu)^2 + y^2}. \end{aligned}$$

The equation of motion is

$$\ddot{z} + 2i\dot{z} - z = -(1-\mu)\frac{z+\mu}{\rho_1^3} - \mu\frac{z-1+\mu}{\rho_2^3}$$

that is

$$\ddot{x} - 2\dot{y} - x = \frac{\partial V}{\partial x}\,, \quad \ddot{y} + 2\dot{x} - y = \frac{\partial V}{\partial y}\,,$$

where $-V$ is the potential of the system defined by

$$V = \frac{1-\mu}{\rho_1^3} + \frac{\mu}{\rho_2^3}\cdot$$

The system can be written using Hamiltonian formalism setting

$$q_1 = x, \quad q_2 = y, \quad p_1 = \dot{x} - y, \quad q_2 = \dot{y} + x,$$

and the Hamiltonian describing the motion writes

$$H_0(q_1, q_2, p_1, p_2) = \frac{1}{2}(p_1^2 + p_2^2) + p_1 q_2 - p_2 q_1 - \frac{1-\mu}{\rho_1} - \frac{\mu}{\rho_2}\cdot$$

4.3 Jacobi integral, Hill regions and equilibrium points

The Jacobi integral using Hamiltonian formalism is simply the Hamiltonian H_0 which gives

$$H(x, y, \dot{x} - y, \dot{y} + x) = \frac{\dot{x}^2 + \dot{y}^2}{2} - \Omega(x, y)$$

where

$$\Omega(x, y) = \frac{1}{2}(x^2 + y^2) + \frac{1-\mu}{\rho_1} + \frac{\mu}{\rho_2}\cdot$$

Solutions are confined on the level set

$$\frac{\dot{x}^2 + \dot{y}^2}{2} - \Omega(x, y) = h, \quad h \text{ constant.}$$

The *Hill domain* for the value h is the region where the motion can occur, that is $\{(x, y) \in \mathbf{R}^2 \mid \Omega(x, y) + h \geq 0\}$.

The equilibrium points of the problem are well known. They split into two different types:

– *Euler points.* They are the collinear points denoted L_1, L_2 and L_3 located on the line $y = 0$ defined by the primaries. For the Earth-Moon problem they are given by

$$x_1 \simeq -1.0051, \quad x_2 \simeq 8.369e-1, \quad x_3 \simeq 1.1557.$$

– *Lagrange points.* The two points L_4 and L_5 form with the two primaries an equilateral triangle.

Some important information about stability of the equilibrium points are provided by the eigenvalues of the linearized system. The linearized matrix evaluated at points L_1, L_2 or L_3 admits two real eigenvalues, one being strictly positive, and two imaginary ones. The collinear points are consequently not stable. In particular, the eigenvalues of the linearized matrix evaluated at L_2 with $\mu = 1.2153e-2$ are approximately ± 2.931837 and $\pm 2.334248i$. When it is evaluated at L_4 or L_5, the linearized matrix has two imaginary eigenvalues since $\mu < \mu_1 = (1/2)(1 - \sqrt{69}/9)$ in the Earth-Moon system. Points L_4 and L_5 are thus stable according to Arnold stability theorem [24]. See also [23] for a review of mission design techniques using the equilibrium points.

4.4 The continuation method

The mathematical continuation method in the restricted circular problem is omnipresent in Poincaré's work, in particular for the continuation of circular orbits [25]. Geometrically, it is simply a continuation of trajectories of Kepler problem into trajectories of the 3-body problem. It amounts to considering μ as a small parameter—the limit case $\mu = 0$ being Kepler problem in the rotating frame—writing

$$H_0 = \frac{|p|^2}{2} - {}^t qKp - \frac{1}{|q|} + o(\mu).$$

The approximation for μ is valid, a neighbourhood of the primaries being excluded. In the Earth-Moon problem, since μ is very small, the Kepler problem is a good approximation of the motion in a large neighbourhood of the Earth. This point of view is important in our analysis, as indicated by the status report of the SMART-1 mission since most of the mission time is spent under the influence of the Earth attraction only, see [28, 29].

4.4.1 The control problem

The control system in the rotating frame is deduced from the previous model and can be written in Hamiltonian form

$$\frac{\mathrm{d}x}{\mathrm{d}t} = \overrightarrow{H}_0(x) + u_1 \overrightarrow{H}_1(x) + u_2 \overrightarrow{H}_2(x)$$

where $x = (q, p)$, $\overrightarrow{H}_0$ is the free motion and $\overrightarrow{H}_1$,$\overrightarrow{H}_2$ are given by $\overrightarrow{H}_i = -q_i$, i =1,2. As for the Kepler problem, the mass variation of the satellite can be introduced in the model dividing u_i by $m(t)$ and adding the equation $\dot{m} = -\delta|u|$. Again, it will be not taken into account here. Moreover we still restrict our analysis to the energy minimization problem with fixed final time t_f and control

valued in $\mathbf{R}^2$. The physical problem which is to maximize the final mass can be analyzed using a continuation method.

A lunar mission using low propulsion called SMART-1 was realized by ESA and the practical details of the mission—in particular the description of the trajectory—are reported in [29]. We present a trajectory analysis based on our geometric and numerical techniques. For simplicity, we have fixed the boundary conditions to circular orbits, the one around the Earth corresponding to the geostationary one. But everything can be applied to other boundary conditions, for instance those described in the report status of the SMART-1 mission. A trajectory comparison is discussed in the final section (see also [6]).

Our analysis is based on a numerical continuation, including second-order optimality check, where μ is the parameter of the continuation. The averaged system is finally applied to get an approximate energy minimizing trajectory for the phase of the mission that starts from the circular Earth orbit and aims at a quasi-elliptic orbit where the apogee is about 338000 Kilometers. In the restricted problem approximation, the effect of the inclination (around 30 degrees in phase two of the mission) is not modelled here.

4.4.2 Numerical continuation for the Earth-L_2 transfer

As a first approach we choose to simulate the Earth-L_2 transfer in the restricted 3-body problem. Indeed, in the limit case $\mu = 0$, the Moon and the point L_2 are identical. Moreover, in the Earth-Moon system, the point L_2 and the Moon are very close. As a result, the first phase of an Earth-Moon transfer is comparable to an Earth-L_2 transfer. Solving the shooting function associated with the Earth-L_2 transfer is consequently useful to provide a good approximation of the solution of the Earth-Moon transfer shooting function.

Using a circular orbit around the Earth for the geostationary one, we set as initial condition $x_0 = (1 - \mu + 1.099e - 1, 0, 0, 2.8792)$. The point L_2 is located on $(x_{L_2}, 0)$ with x_{L_2} solution of the equation

$$x - \frac{(1-\mu)(x+\mu)}{\rho_1^3} - \frac{\mu(x-1+\mu)}{\rho_2^3} = 0.$$

Since we want to reach L_2 with a zero speed, we fix the target $x_f = (x_{L_2}, 0, 0, 0)$. By making the parameter μ vary from zero, one builds up a family $(S_\mu)_\mu$ of shooting functions which connects the Kepler and the 3-body problem. The numerical continuation method can be applied to deduce low thrust extremal trajectories of the Earth-L_2 transfer from the Kepler ones.

In accordance with the report status of ESA, we fix the transfer time to 121 time units of the restricted 3-body problem, which approximately corresponds to the transfer time from the Earth to the point L_2 during the SMART-1 mission (about 17 months). In addition, we consider a constant spacecraft mass of 350 Kilograms, see [28, 29]. Setting $\mu = 0$, we compute an extremal using the shooting method, then increase μ up to $1.2153e-2$ with a discrete continuation. At each step, the first conjugate time along the extremal is computed to ensure convergence of the continuation method. The Euclidian norm of the extremal control is plotted Fig. 14 to draw a comparison between the control bound and the maximum thrust allowed by electro-ionic engines. Figs. 7 to 14 present the computed spacecraft trajectories in both rotating and fixed frames, as well as

the first conjugate time and the norm of the control along trajectories in Kepler and Earth-Moon systems.

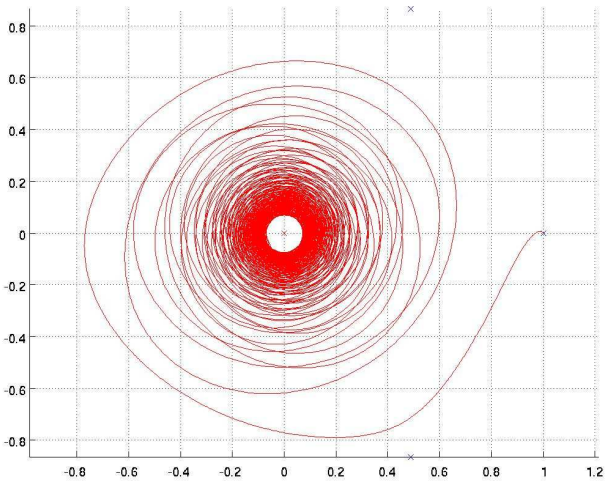

Figure 7: Earth-L_2 trajectory in the rotating frame, $\mu = 0$.

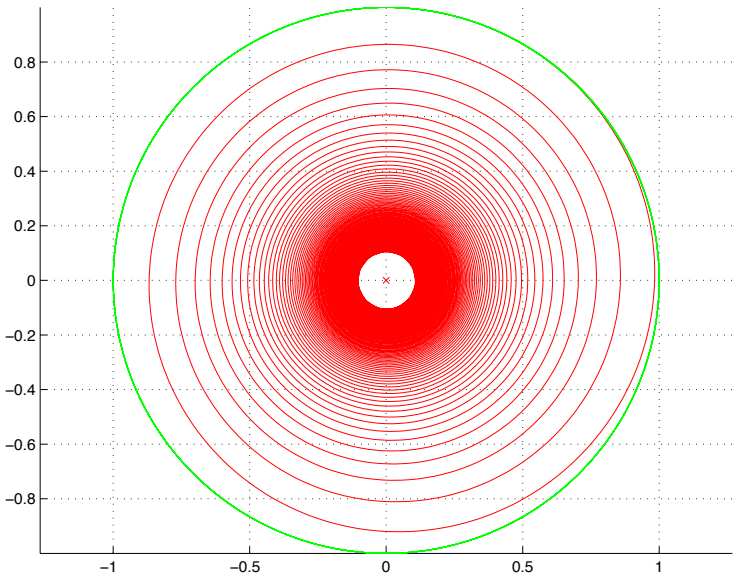

Figure 8: Earth-L_2 trajectory in the fixed frame, $\mu = 0$.

The numerical continuation method, considering μ as a small parameter, leads to deduce an extremal trajectory of the energy minimization Earth-L_2 transfer problem from one corresponding to the Kepler case, in accordance with

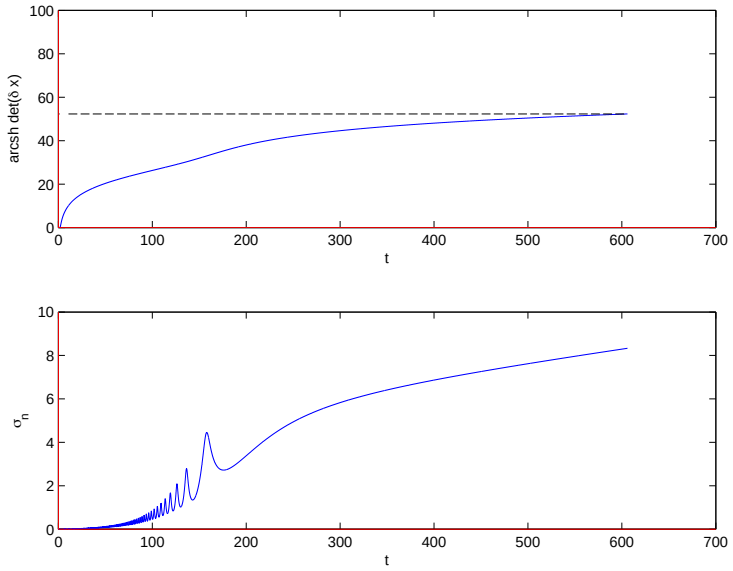

Figure 9: First conjugate time, Earth-L_2 transfer, $\mu = 0$.

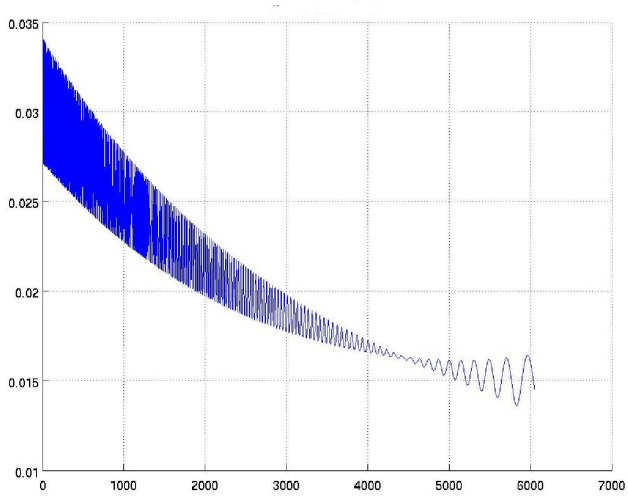

Figure 10: Norm of the extremal control, Earth-L_2 transfer, $\mu = 0$.

Poincaré's work. The second order optimality condition check ensure that the computed extremals are locally energy minimizing in $\mathrm{L}^\infty([0, t_f])$. We also note that in both cases $\mu = 0$ and $\mu = 1.2153e-2$, the maximum value reached by the norm of the extremal control is inferior to the bound $|u| \leq 8e-2$ of the SMART-1 electro-ionic engine ($7.3e-2$ Newtons), while transfer times are comparable.

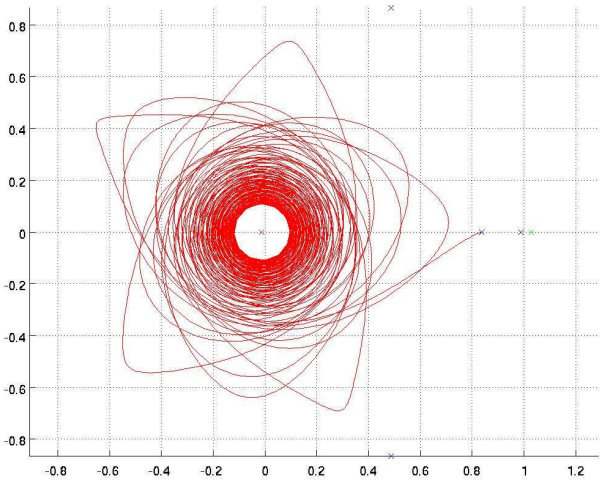

Figure 11: Earth-L_2 trajectory in the rotating frame, $\mu = 1.2153 - 2$.

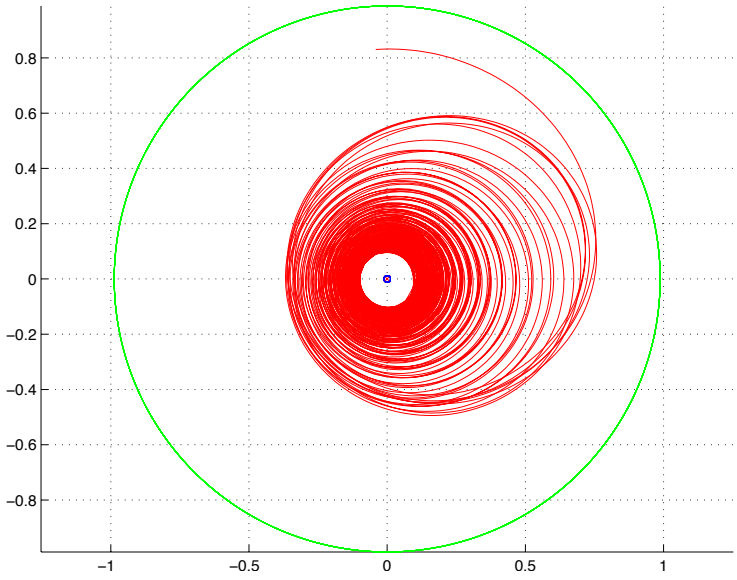

Figure 12: Earth-L_2 trajectory in the fixed frame, $\mu = 1.2153e - 2$.

4.4.3 Numerical continuation method for the Earth-Moon transfer

The second part of our trajectory analysis is devoted to the Earth-Moon transfer. We use the same dynamics and initial conditions as previously. In this case, the circular orbit around the Moon, denoted O_L and defined by

$$(x_1 - 1 + \mu)^2 + x_2^2 = 1.7e-3, \quad x_3^2 + x_4^2 = 2.946e-1, \quad (x_1 - 1 + \mu, x_2) \perp (x_3, x_4),$$

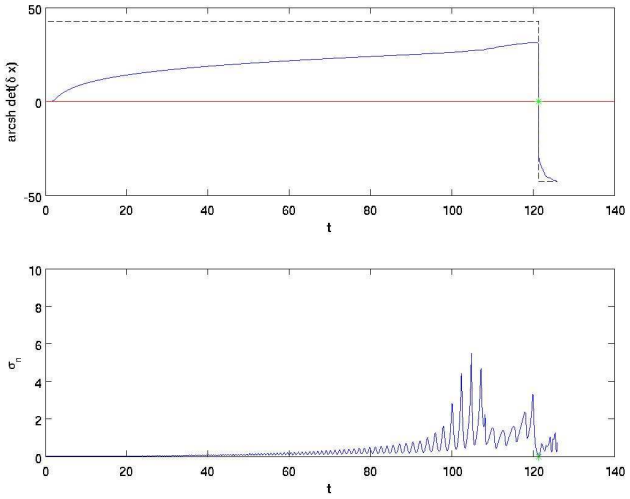

Figure 13: First conjugate time, Earth-L_2 transfer, $\mu = 1.2153e-2$.

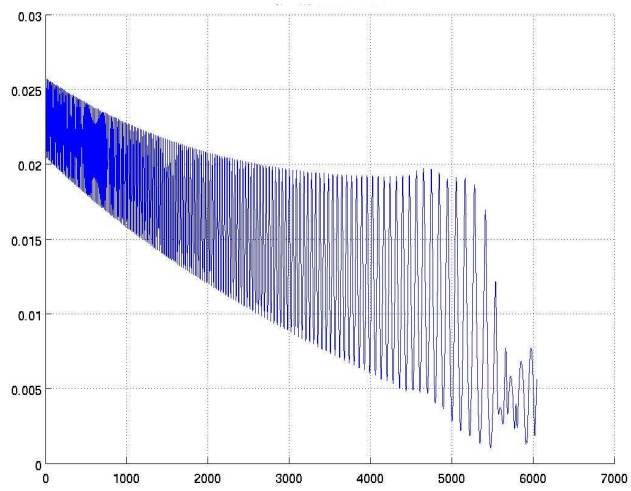

Figure 14: Norm of the extremal control, Earth-L_2 transfer, $\mu = 1.2153e-2$.

is chosen as the target orbit. In addition to the former necessary conditions, the maximum principle provides the transversality condition $p(t_f) \perp T_{x(t_f)}O_L$. The shooting equation is modified accordingly, and one has to check local optimality computing focal instead of conjugate points.

The transfer time is fixed to 124 time units of the restricted 3-body problem. The extremal trajectory is obtained using the shooting method and initializing p_0 with the initial costate vector of the Earth-L_2 transfer. The Earth-Moon

trajectories in both rotating and fixed frames, the first focal time and the norm of the extremal control are presented from Fig. 15 to Fig. 22 for μ varying between 0 and $1.2153e-2$. In the two cases $\mu = 0$ and $\mu = 1.2153e-2$, the first focal time along extremals $t_{1,\mathrm{foc}}$ is higher than $3t_f/2$, ensuring local optimality. The maximal bound of the norm of the extremal control is about $4.5e-2$ which approximately corresponds to the half of the maximal thrust allowed during SMART-1 mission.

It is interesting to notice that the Earth-L_2 Keplerian trajectory differs from the Earth-Moon Keplerian trajectory. The first phase of the Earth-Moon transfer matches the Earth-L_2 transfer. It underlines the crucial role of the neighbourhood of the point L_2 where the attractions of the two primaries compensate each other. By treating the first phase as a Keplerian transfer from the geostationary orbit (GEO) to a geostationary transfer orbit (GTO), we are able to use the averaging results of section 3.2 in order to estimate the maximal bound of the control associated with energy minimizing trajectories.

The first phase of the Earth-Moon trajectory with $\mu = 1.2153e-2$ can be approximated by a Keplerian transfer from the GEO to a GTO orbit with semi-major axis $a \simeq 5.84e-1$, eccentricity $e \simeq 3.96e-1$, and argument of pericenter $\theta = 8\pi/7$. Using the system of coordinates introduced in Proposition 3.9, one can compute the appropriate geodesic and estimate the final longitude required to achieve a prescribed maximal bound on the norm of the control thanks to Proposition 3.7.

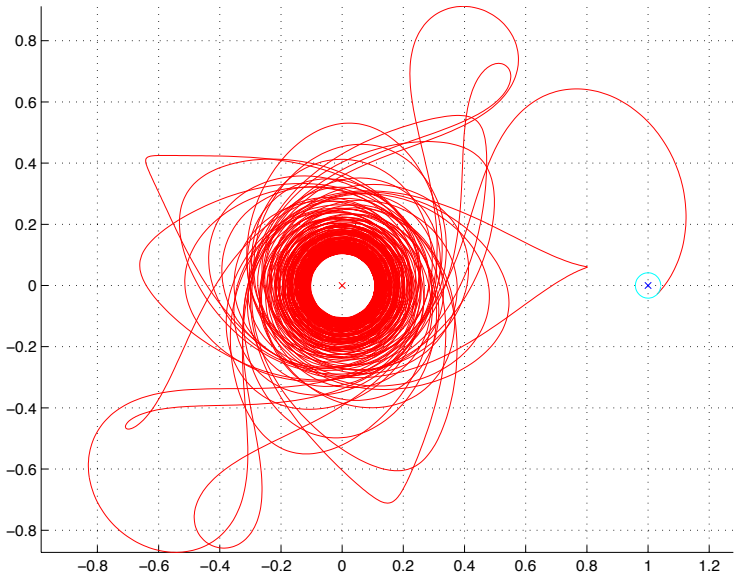

Figure 15: Earth-Moon trajectory in the rotating frame, $\mu = 0$.

References

[1] Allgower, E. L.; Georg, K. *Numerical continuation methods, an introduction*. Springer, Berlin, 1990.

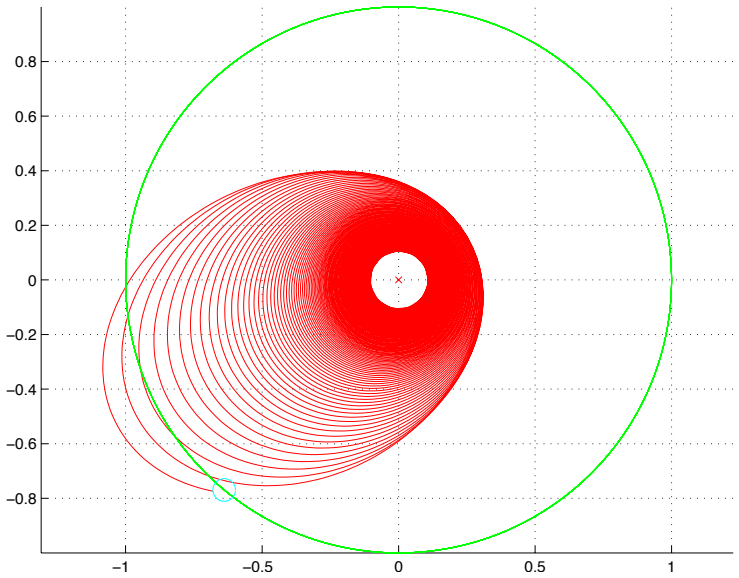

Figure 16: Earth-Moon trajectory in the fixed frame, $\mu = 0$.

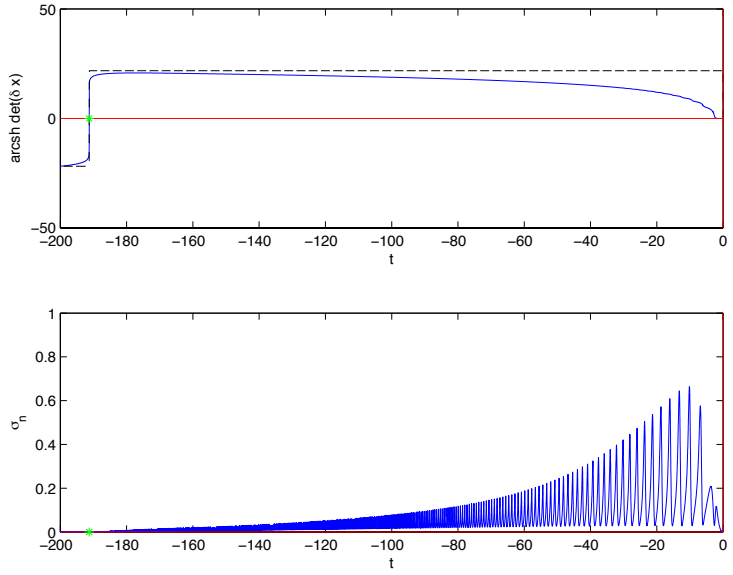

Figure 17: First focal time and norm of extremal control, Earth-Moon transfer, $\mu = 0$.

[2] Arnold, V. I. *Mathematical methods of classical mechanics*. Springer, New-York, 1989.

[3] Bellaïche, A. The tangent space in sub-Riemannian geometry. *Sub-Riemannian geometry*, 1–78, Progr. Math. **144**, Birkhäuser, 1996.

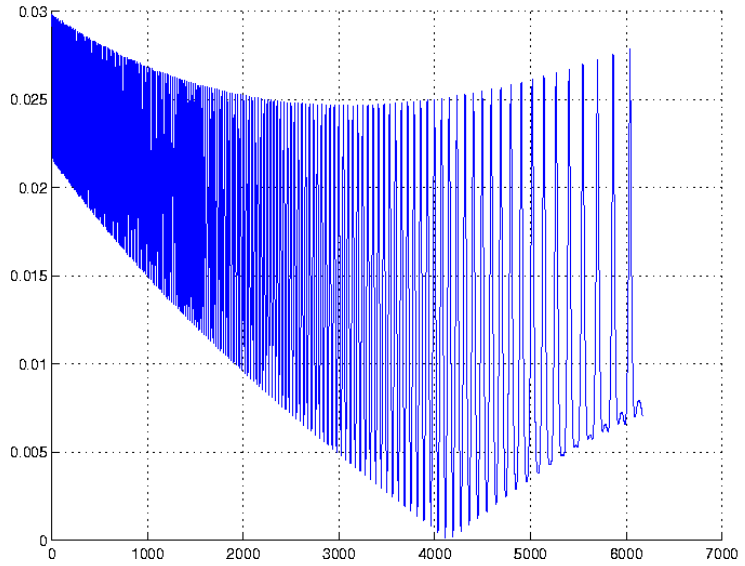

Figure 18: Norm of extremal control, Earth-Moon transfer, $\mu = 0$.

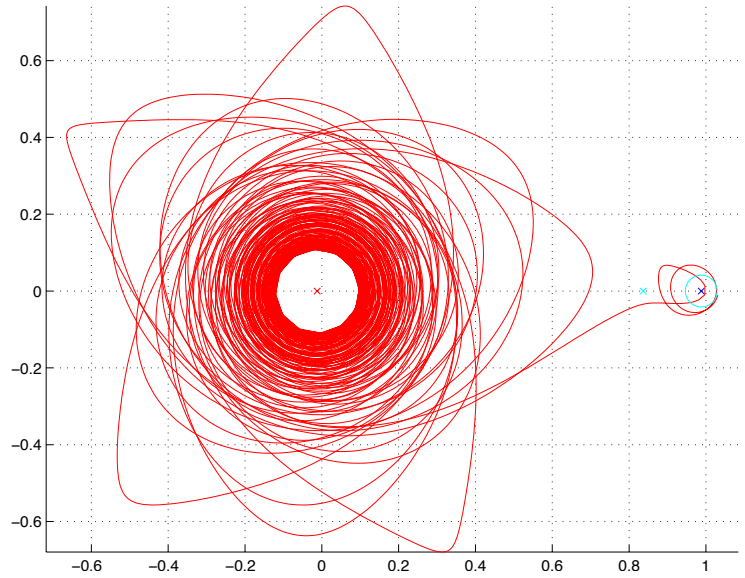

Figure 19: Earth-Moon trajectory in the rotating frame, $\mu = 1.2153e - 2$.

[4] Bensoussan, A. Regular perturbations in optimal control. *Singular perturbations in systems and control* (Udine, 1982), 169–183, CISM Courses and Lectures, 280, Springer, Vienna, 1983.

[5] Bliss, G. A. *Lectures on the Calculus of Variations*. Chicago, 1946.

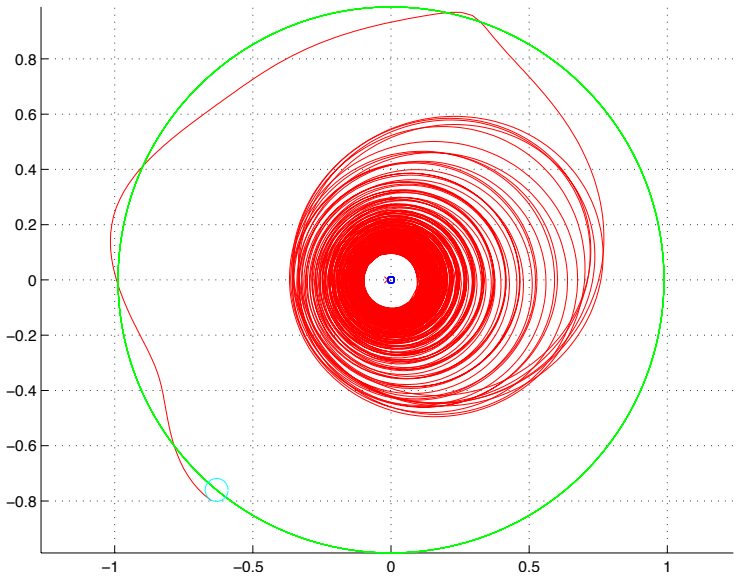

Figure 20: Earth-Moon trajectory in the fixed frame, $\mu = 1.2153e-2$.

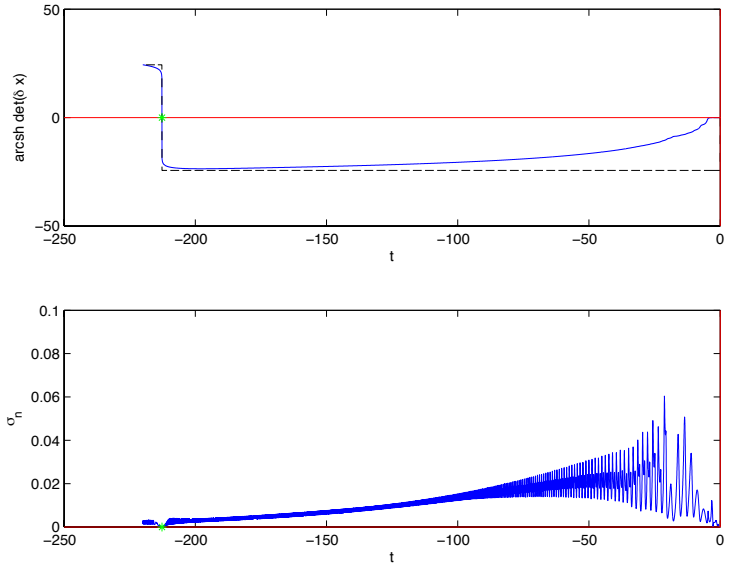

Figure 21: First focal time, Earth-Moon transfer, $\mu = 1.2153e-2$.

[6] Bombrun, A.; Chetboun, J.; Pomet, J.-B. Transfert Terre-Lune en poussée faible par contrôle feedback – La mission SMART-1. *INRIA Research report* (2006), no. 5955, 1–27.

[7] Bonnard, B.; Caillau, J.-B. Riemannian metric of the averaged energy minimization problem in orbital transfer with low thrust. *Ann. Inst. H. Poincaré*

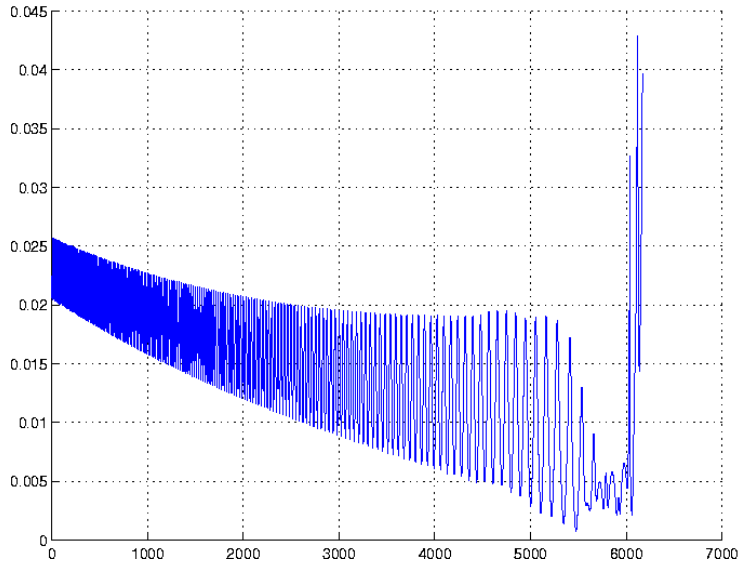

Figure 22: Norm of extremal control, Earth-Moon transfer, $\mu = 1.2153e - 2$.

Anal. Non Linéaire **24** (2007), no. 3, 395–411.

[8] Bonnard, B.; Caillau, J.-B. Geodesic flow of the averaged controlled Kepler equation. *Forum math.* **21** (2009), no. 5, 797–814.

[9] Bonnard, B; Caillau, J.-B. Singular metrics on the two-sphere in space mechanics. *HAL preprint* (2008), no. 00319299, 1–25.

[10] Bonnard, B.; Caillau, J.-B.; Dujol, R. Energy minimization of single-input orbit transfer by averaging and continuation. *Bull. Sci. Math.* **130** (2006), no. 8, 707–719.

[11] Bonnard, B.; Caillau, J.-B.; Sinclair, R.; Tanaka, M. Conjugate and cut loci of a two-sphere of revolution with application to optimal control. *Ann. Inst. H. Poincaré Anal. Non Linéaire* **26** (2009), no. 4, 1081–1098.

[12] Bonnard, B.; Caillau, J.-B.; Trélat, E. Second order optimality conditions in the smooth case and applications in optimal control. *ESAIM Control Optim. and Calc. Var.* **13** (2007), no. 2, 207–236 (`apo.enseeiht.fr/cotcot`).

[13] Bonnard, B.; Shcherbakova, N.; Sugny, D. The smooth continuation method in optimal control with an application to control systems. *ESAIM Control Optim. and Calc. Var*, to appear.

[14] Caillau, J.-B. *Contribution à l'étude du contrôle en temps minimal des transferts orbitaux*. Phd thesis, Toulouse Univ., 2000.

[15] Chaplais, F. Averaging and deterministic optimal control. *SIAM J. Control Optim.* **25** (1987), no. 3, 767–780.

[16] Do Carmo, M. P. *Riemannian geometry*. Birkhäuser, Boston, 1992.

[17] Edelbaum, T. N. Optimal low-thrust rendez-vous and station keeping. *AIAA J.* **2** (1964), no. 7, 1196–1201.

[18] Geffroy, S. *Généralisation des techniques de moyennation en contrôle optimal. Application aux problèmes de transfert et rendez-vous orbitaux à poussée faible*. Phd thesis, Toulouse Univ., 1997.

[19] Gergaud, J.; Haberkorn, T. Homotopy method for minimum consumption orbit transfer problem. *ESAIM Control Optim. Calc. Var.* **12** (2006), no. 2, 294–310.

[20] Guckenheimer, J.; Holmes, P. *Nonlinear oscillations, dynamical systems and bifurcations of vector fields*. Springer, 1993.

[21] Guerra, M.; Sarychev, A. Existence and Lipschitzian regularity for relaxed minimizers. *Mathematical control theory and finance*, 231–250, Springer, Berlin, 2008.

[22] Kato, T. *Perturbation theory for linear operators*. Springer, 1980.

[23] Marsden, J. E.; Ross, S. D. New methods in celestial mechanics and mission design, *Bull. Amer. Math. Soc. (N.S.)* **43** (2006), no. 1, 43–73.

[24] Meyer, K.; Hall, G. R. *Introduction to Hamiltonian dynamical systems and the N-body problem*. Springer, New York, 1992.

[25] Poincaré, H. *Oeuvres*. Gauthier-Villars, Paris, 1934.

[26] Pollard, H. *Mathematical introduction to celestial mechanics*. Prentice-Hall, Englewood Cliffs, 1966.

[27] Pontryagin, L. S.; Boltyanskii, V. G.; Gamkrelidze, R. V.; Mishchenko, E. F. *The mathematical theory of optimal processes*. John Wiley & Sons, New York, 1962.

[28] Racca, G.; Foing, B. H.; Coradini, M. SMART-1: The first time of Europe to the Moon. *Earth, Moon and planets* **85-86** (2001), 379–390.

[29] Racca, G.; *et al.* SMART-1 mission description and development status. *Planetary and space science* **50** (2002), 1323–1337.

[30] Sinclair, R.; Tanaka, M. The cut locus of a two-sphere of revolution and Toponogov's comparison theorem. *Tohoku Math. J.* **59** (2007), no. 2, 379–399.

[31] Szebehely, V. *Theory of orbits: The restricted problem of three bodies*. Academic Press, 1967.